ZORN, KIMBERLEY M., M.S. Construction of a Synaptic Membrane for *in silico* Endocannabinoid Investigations. (2016)
Directed by Dr. Patricia H. Reggio. 53 pp.

The mechanism of a chemical reaction cannot be assumed prior to identifying the solvent, thus to accurately model membrane-bound cannabinoid receptors, details of the lipid bilayer must be considered as well. Traditionally thought of as a permeable barrier, the membrane also serves as a medium for hydrophobic ligand delivery; the Reggio group has published on the entry of *sn*-2-arachidonoylglycerol into the cannabinoid CB2 receptor through the trans-membrane region. Currently receptor and ligand trajectories are calculated in a single-phospholipid bilayer, however biological membranes are comprised of many lipid species. Herein nanosecond timescale molecular dynamics studies of various membrane compositions are reported, culminating to a final model mimicking a synaptic plasma membrane in phospholipid composition. Structural changes to phospholipids in increasingly heterogeneous compositions are discussed, along with interactions between endocannabinoid *N*-arachidonoylglycine (NAGly) and membrane components. The final model provides a significant contrast to a pure phosphatidylcholine bilayer, in addition to proposing new investigations of ligand diffusion, phospholipid clustering, and similar hydrogen bonding studies.

CONSTRUCTION OF A SYNAPTIC MEMBRANE FOR *IN SILICO* ENDOCANNABINOID INVESTIGATIONS

by

Kimberley M. Zorn

A Thesis Submitted to
the Faculty of The Graduate School at
The University of North Carolina at Greensboro
in Partial Fulfillment
of the Requirements for the Degree
Master of Science

Greensboro
2016

Approved by

Patricia H. Reggio
Committee Chair

APPROVAL PAGE

This thesis, written by Kimberley M. Zorn, has been approved by the following committee of the Faculty of The Graduate School at The University of North Carolina at Greensboro.

Committee Chair	Patricia H. Reggio
Committee Members	Alice Haddy
	Jason Reddick

November 2, 2016
Date of Acceptance by Committee

November 2, 2016
Date of Final Oral Examination

TABLE OF CONTENTS

Page

LIST OF TABLES

Page

LIST OF FIGURES

Page

CHAPTER I

INTRODUCTION

Overview of Cell Membrane Diversity

Despite the vast diversity of components and function between organisms, cell membrane structure is described with the Fluid Mosaic Model,[1] featuring the familiar two-dimensional bilayer of phospholipids surrounding protein 'islands'. In the past, the Fluid Mosaic Model was a groundbreaking explanation of available experimental data, based on a relatively simple thermodynamic argument: a phospholipid bilayer maximizes both hydrophobic and hydrophilic interactions, minimizing the total free energy. Currently, the Fluid Mosaic Model is widely accepted, but at the time of publication some were skeptical of making any generalizations about membrane structure, partially due to the overwhelming diversity of lipid components.

Skepticism of the Fluid Mosaic Model is understandable, since the proportions of lipid species between plasma membranes of different organisms are strikingly dissimilar. Examination of the chemical details between membrane compositions exemplifies that while the bilayer structure is universal, a specific lipid composition accompanies a particular function. Bacterial phospholipids contain cyclopropyl rings in the fatty acid chains, but these moieties are absent in mammalian membranes;[2] intracellularly, there are also marked increased in specific phospholipids of different organelles in yeast.[3]

Furthermore, the concentration of anionic phospholipids in yeast is increased compared to mammalian cells.[4] Even within the human body, cell types have contrasting lipid proportions associated with optimal function. Liver cell plasma membranes contain more cholesterol than those of red blood cells,[5,6] but both cell types lack the highly olefinated fatty acids that are characteristic of nerve cells.[7,8]

Investigation of the cannabinoids in the central nervous system is of paramount importance, known already to have influence in hunger, memory, and mood.[9,10] The structure of a membrane-bound protein requires a consideration of the native environment. Cannabinoid subtype 1 receptor (CB1) is native to a presynaptic neuronal plasma membrane.[10] The exact composition of neuronal plasma membranes is lacking, but there are published proportions of phospholipid moieties of synaptic membranes.[7,8] Combined with known features of mammalian plasma membranes,[4] there is sufficient information to develop a suitable model of a neuronal plasma membrane.

Membrane Lipids *in vivo*

The balls and sticks in the Fluid Mosaic Model are a representation of a glycero-phospholipid; a basic structure of this lipid is shown in Figure 1A. These phospholipids have a glycerol core composed of three carbons, referred to as the *sn*-1, -2 and -3 positions in phospholipid stereospecific nomenclature.[11] The *sn*-1 and *sn*-2 positions occupy esterified fatty acids; the former is usually saturated and the latter olefinated, and the *sn*-3 position links the phosphate head-group which defines each species. Pertinent glycero-phospholipid species in mammalian membranes include phosphatidylcholine, phosphatidylserine, phosphatidylethanolamine and phosphatidylinositol-biphosphates.

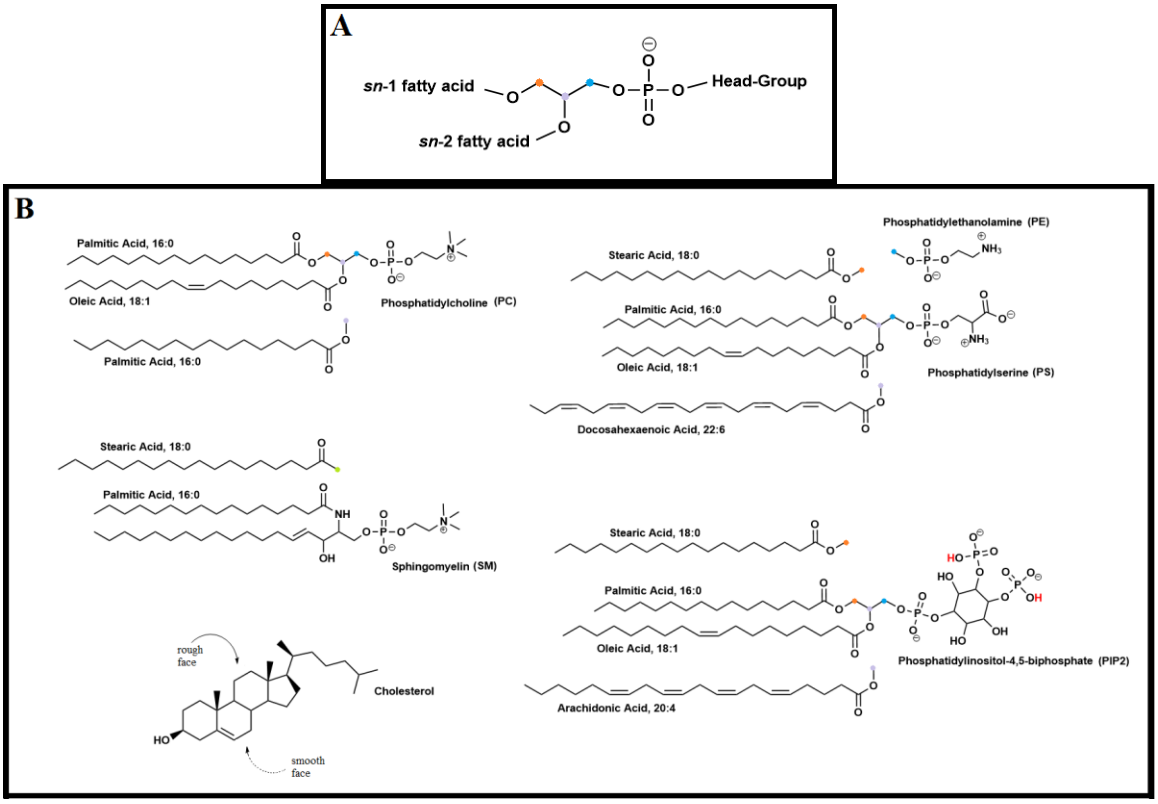

Figure 1. Lipid Library. (A) The basic structure of a glycero-phospholipid. (B) Lipid library of all membrane components. Both head-group and acyl chains are labelled, with carbon:olefins. Ethanolamine and serine phospholipids have identical fatty acids. Acyl chains of all phospholipid were palmitic and oleic acid in Bilayers 0-4.

All glycero-phospholipid species chemical structures are shown in Figure 1B. Choline, a quaternary ammonium cation, is the most common phospholipid head-group in eukaryotic plasma membranes.[4] The stifled hydrogen bond donating capability of choline and its steric bulk prevent intramolecular hydrogen bonds with anionic phosphates, limiting lateral packing in bilayers.[12] Without canonical hydrogen bonding, a network of water molecules reduce electrostatic repulsion between phosphates in a pure phosphatidylcholine bilayer.[11] This is in contrast to ethanolamine, a demethylated analog

of choline; the small primary amine forms tight hydrogen bonding networks with adjacent phosphates and forms a hexagonal phase structure at melting temperature rather than a planar bilayer structure.[13,14] This distinct phase behavior implicates phosphatidylethanolamine in membrane curvature[14] and vesicle budding.[4] Phosphatidylethanolamine is present in the extracellular leaflet, but concentrated in the cytosolic leaflet of mammalian plasma membranes.[4,14] Serine contains a primary amine and a carboxylate, zwitterionic at biological pH; this dual hydrogen bonding potential restricts head-group motion compared to ethanolamine or choline.[12] Phosphatidylserine is almost exclusively located in the cytosolic leaflet of healthy mammalian membranes[4,14] and has been implicated in recruiting cholesterol to the cytosolic leaflet[15] as well as proteins to the membrane surface.[16] Inositol phospholipids have a vast functional repertoire, serving as enzymatic cofactors, precursor to messengers, and a recruiter of proteins to the membrane surface.[4,17] In molecular dynamics simulations of the dopamine transporter, phosphatidylinositol-4,5-bisphosphate interacts with the transporter N-terminus to promote an inward-facing opening.[18] While it is of paramount physiological importance, phosphatidylinositol-4,5-bisphosphate is tightly controlled the cell as a minute percentage of mammalian membranes.[4,14,19]

Below the water-interface, fatty acids of phospholipids dictate the inner, hydrophobic environment of the lipid bilayer. Long, saturated hydrocarbon chains tend to extend and pack together tightly through van der Waals forces, while c*is* olefins invoke chain bending and maintain the fluidity of the bilayer via mild destabilization of packing.[20,21] Polyunsaturated fatty acids, long acyl chains contain multiple homo-allylic

double bonds, and are common in phosphatidylserine, phosphatidylethanolamine and phosphatidylinositol lipid species in synaptic plasma membranes.[7,8] Omega-3 fatty acids like docosahexaenoic acid are not made *in vivo* but have been found to be essential for optimal CB1 function in mice,[9] and are concentrated in the visual system.

Sphingomyelin was also included in the heterogeneous membrane model, structure shown in Figure 1B. While it is a phospholipid, it contrasts with the previous mentioned species in that it is linked to a sphingosine rather than glycerol core; in general sphingomyelin contains a long, saturated fatty acid.[4,22] Sphingomyelin is more concentrated in the extracellular leaflet of membranes,[4] and more abundant in myelin[7,8] and red blood cells[6] compared to synaptic membranes. In particular, sphingomyelin packs well against the smooth face of cholesterol, and additional hydrogen bond donors in ceramide further promotes tight packing; lateral segregation of these lipids into rafts of restricted acyl chain movement and increased hydrophobic thickness.[22] While is it not uncommon for sphingomyelin to have an ethanolamine head-group, herein sphingomyelin contains a choline head-group.

In mammalian cells, cholesterol, structure also shown in Figure 1B, can reach up to 50% depending on location.[4,14] Cholesterol in bilayers has an area condensation effect, decreasing the lateral surface area of phospholipid components.[23,24] Increasing unsaturation in phospholipids diminishes this effect due to the non-ideal hydrophobic packing.[20–23] In general, fully or minimally saturated phospholipid bilayers have cholesterol molecules positioned upright with the hydroxyl facing the water interface, as shown in Figure 2A. Mixed-chain phospholipids have directional specificity emphasizing

the preference of cholesterol, packing saturated fatty acids against the sterol and orienting polyunsaturated chains toward bulk lipid.[20] Cholesterol has also been found to reside in the center of di-polyunsaturated and thin phospholipid bilayers, with the hydroxyl in the methyl region of the bilayer, as shown in Figure 2B.[25–27]

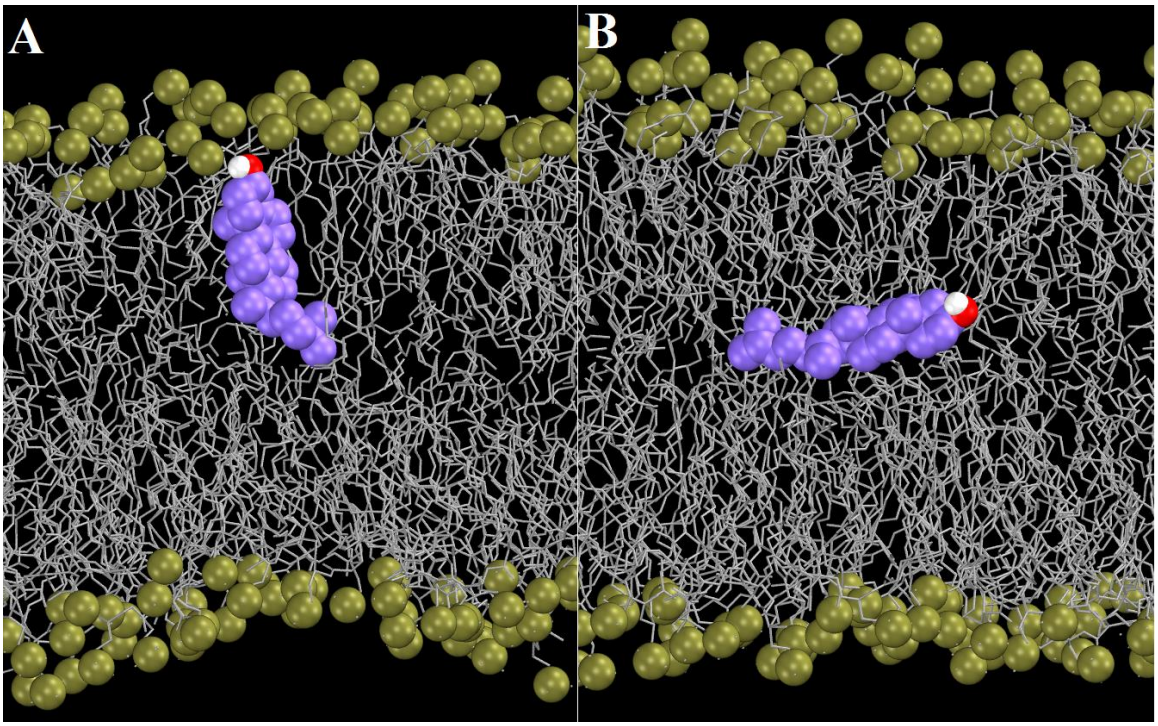

Figure 2. Positions of Cholesterol in the Bilayer. (A) Upright and (B) horizontal in the center of the bilayer., cholesterol carbons in violet, oxygen in red and hydrogen in white. Phosphorus atoms of phospholipids are shown in gold spheres, and acyl chains are shown by silver sticks. Some lipids and all nonpolar hydrogens are omitted for clarity.

Cholesterol is not completely limited to one position or the other, but rather is always in dynamic movement in the hydrophobic core; orientation is favored by minimizing contact with water. Translocation of cholesterol between leaflets, or flip-flop, has been observed in simulations of both saturated and polyunsaturated bilayers.[26,28–31]

in silico Modeling of Membranes

When developing a chemical reaction one would not assume a mechanism without identifying the solvent, since it can greatly impact the mechanism. Similarly, the membrane lipids surrounding G-protein-coupled receptors (GPCRs) are essential to accurately dissect the mechanism of their activation. GPCR is a general term for a variety of transmembrane receptors that regulate intracellular signaling via G-proteins. In general, GPCR structural research has been limited by the difficulties associated with crystallization of native transmembrane receptors; the removal of receptors from the bilayer is associated with loss of function and structural defects.[14] A protein crystal structure is merely a snapshot in time rather than a gold-standard of dynamic *in vivo* structure, like comparing a frozen and rotisserie chicken. However, both static and dynamic computational, *in silico*, models of GPCRs can assist in structure-activity relationships. Amino acid sequences are known, and thus conformational considerations can be applied to solve the native structure of a receptor; though theoretical in nature, *in silico* models can bolster a hypothesis by identifying specific ligand-receptor interactions that can be tested experimentally.

Computational models of plasma membranes have become more prominent with the advancement of technology. Ingólfsson et al. published results on a significantly large bilayer consisting of over sixty phospholipid species.[30] However, their coarse-grained simulation methods omit atomistic detail to improve computational feasibility. Therefore precise, all-atom simulation methods remain imperative. In 2016, Andoh et al. investigated the structure of a bilayer based on diseased and healthy liver cell membrane

compositions made up of several phospholipids.[5] They found that the diseased state reduced the fluidity of the bilayer, and demonstrated the effect of lipid composition on structure and consequently function of the plasma membrane. Recent updates to parameters of oxygen-sodium interactions,[32] sphingomyelin,[33] and polyunsaturated fatty acids[34] mean an *in silico* model of a heterogeneous membrane can be more accurate than ever before.

The Reggio group has published work on the role of the membrane in GPCRs activation, such as ligand hydrogen bonding patterns with phospholipids,[35,36] endocannabinoid activation of the receptor binding pocket through a transmembrane portal,[37] and have simulated the entry of various ligands into a lipid bilayer. However, the bilayer surrounding a given receptor has always been composed of a single phospholipid species. In an effort to create a more accurate model of a GPCR assembly in the brain, the membrane surrounding the receptor should also model the native membrane environment. Prior to the insertion of a GPCR into the membrane, it is pertinent to evaluate how the behavior of a ligand will be altered in a heterogeneous membrane.

N-arachidonoylglycine

The lipophilic endocannabinoid *N*-arachidonoylglycine (NAGly) was found to be the endogenous ligand of putative cannabinoid receptor GPR18.[38] Similar to anandamide (AEA) and *sn*-2-arachidonylglycerol, NAGly contains an arachidonic acid scaffold, studied extensively by the Reggio group, however unlike AEA, NAGly is negatively charged at physiological pH, as shown in Figure 3.

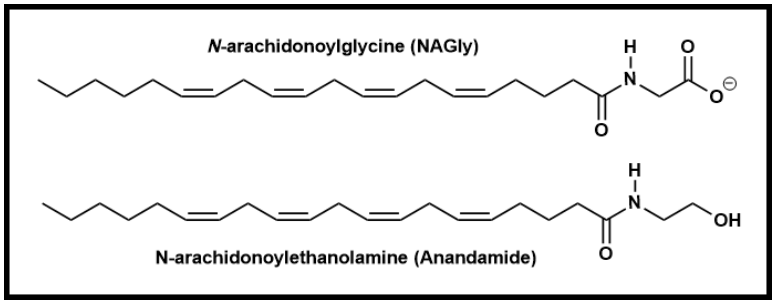

Figure 3. Structures of NAGly and AEA.

The Conformational Memories method is a means of calculating low-energy conformers of flexible compounds at biological temperature. This method consists of Monte Carlo/simulated annealing random walks evaluating torsional freedom of the molecule over 310-3000 K.[39] The exploratory phase calculates dihedral distributions over the entire temperature range, and the biased phase samples only regions of conformational space shown to be populated in the previous phase, over a smaller temperature range of 710-310 K. In a variety of solvents,[36,40] this method has shown arachidonic acid takes on predominately extended and U-shapes, as shown in Figure 4.

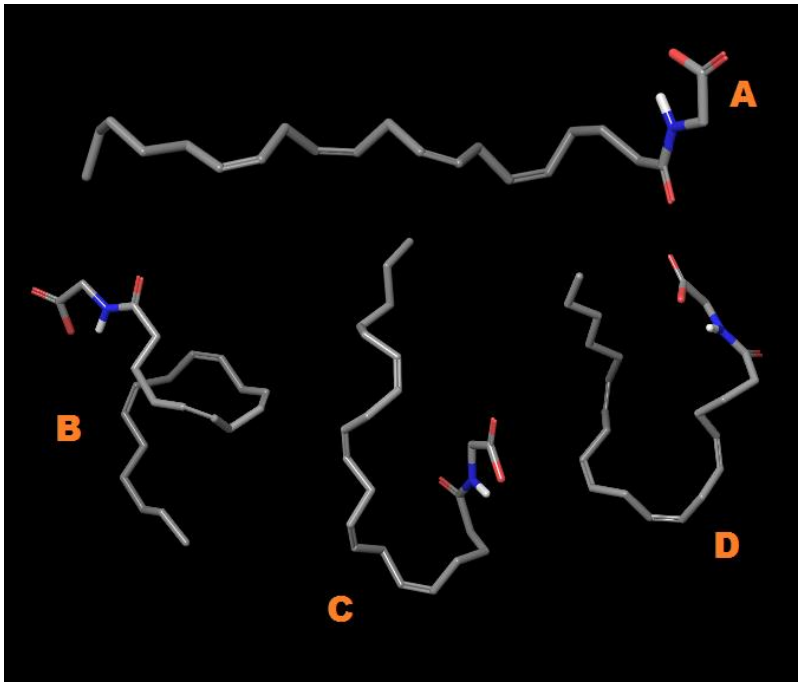

Figure 4. Shapes of NAGly. (A) Extended shape, (B) Helical shape, (C) J-shape, and (D) U-shape conformations of arachidonic acid chain in NAGly.

Simulations of *sn*-2-arachidonylglycerol have demonstrated that lipid derived ligands enters the cannabinoid subtype 2 receptor (CB2) through a portal in the transmembrane helices, using the lipid bilayer as a transport medium.[37] Due to the role of the lipid bilayer in the delivery of endocannabinoids, hydrogen bonding trends are pertinent to understand how hydrophilic interactions affect a ligand's ability to reach a target receptor. Studies of small molecules like ethanol[41] and anesthetic compounds[42] have investigated membrane-ligand interactions and how such perturbations can affect bilayer structure and permeability. However, these studies are conducted with hydrophobic compounds, so membrane investigations of lipophilic compounds are significant to add to the body of literature.

Hydrogen bonding patterns of AEA with phospholipids and water have also been investigated by the Reggio group in mono-[35] and di-unsaturated[36] phosphatidylcholine bilayers, discussed in more detail in Chapter IV. Since AEA and NAGly are analogues, the work discussed herein provides an applicable comparison between hydrogen bonding patterns. Hydrogen bonding in a heterogeneous membrane will also provide more insight into the effects of bilayer composition.

Significance & Objectives

The Reggio research group has produced many computational models of GPCRs, mainly confirmed and putative cannabinoid receptors calculated in a single-component membrane. The diversification from this simplistic bilayer is directly significant for computational modeling of GPCR assemblies in the Reggio lab, since studies have shown that specific lipids were essential to the function of CB1 in mice.[9] The *in silico* model of a synaptic membrane is the culmination of several models that systematically increase in compositional complexity. A step-wise diversification of lipid components yielded insight into specific effects on an endocannabinoid hydrogen bonding behavior, as well as ensuring consistency between compositions. Membrane structure and ligand hydrogen bonding studies are directly applicable to GPCR *in silico* modelling, and can propose new biophysical investigations of the role of the membrane *in vivo*.

CHAPTER II

METHODS AND ANALYSIS

Overview of Molecular Dynamics

Static computational models, such as a ligand in the binding pocket of a receptor, are the results of many calculations of rotational energy as well as interaction energy. As the name implies, molecular dynamics simulations model the movement of atoms by extensive derivations of force using a force field, or a collection potential energy functions, to model molecular systems similarly to the ball-and-spring model.[43,44] A force field describes bonded and non-bonded interactions of atoms.[44] Non-bonded interactions are those between two molecules; these require Lennard-Jones parameters, which dictate attraction and repulsion between specific atom pairs.[45] Recently, these parameters were modified for more accurate modeling of phosphatidylserine-sodium interactions in the CHARMM force field.[32] Bonding interactions are intramolecular, defining bond stretching, angle bending, and dihedral terms.[45] A simulation is calculated by repeatedly calculating the force acting on each atom by taking the first-order derivative of potential energy.[43] Subsequently, Newton's equations of motion are applied repeatedly by integrating force over time and recording 3D coordinates of atoms, yielding a molecular dynamics trajectory.[44,45] All-atom simulation methods, defining individual atoms rather than groups of atoms, are more precise but also more time-consuming. The trajectory is then visualized in another software package.

Membrane Construction and Calculation

All bilayer systems are constructed with the Chemistry at HARvard Molecular Mechanics Graphical User Interface (CHARMM-GUI) Membrane Builder.[46] This web-based tool is freely available and utilizes the most recent CHARMM36 all-atom force field, defining precise atomistic interactions instead of united-atom or coarse-grained methods. This tool was used to generate the initial structural, topology, and parameter files necessary for the calculation in NAMD,[47] a superior software for large calculations of biological systems.[45] These input files are generated in a series of five steps through the CHARMM-GUI website. The initial two steps allow the user to select the exact lipid composition of each leaflet based on the extensive lipid library, but stores that information as 'pseudoatom' placeholders, to be replaced later. The third step evaluates the system size and initially packs lipids together by organizing the lipid bilayer with pseudoatoms and standard area per lipids. The fourth step separately constructs the lipid bilayer followed by aqueous layer, including ions. Pseudoatoms are replaced with the previous species selection in step four while detecting any sugar/cholesterol/protein penetration between membrane components. Finally, the fifth step assembles both the bilayer and aqueous layer into one NAMD input system; suggested input files for the trajectory are included based on previous temperature and pressure selections.

Inclusion of a lipophilic ligand in a membrane was not available through CHARMM-GUI, and had to be executed after downloading a similar ligand-free composition. A mixed bilayer composed of phosphatidylserine and phosphatidylcholine was constructed with CHARMM-GUI to initially get an estimate of structural parameters.

Then, phosphatidylserine topology and parameter files were replaced with those for the ligand, created in previous Reggio group conformational searches. Once integrated, the original packing and assembling steps were repeated using CHARMM on UNCG machines to recalculate the initial system construction. After the initial inclusion of NAGly, an area of 58.0 $Å^2$ was used for lateral area per lipid in subsequent compositions including NAGly. In subsequent membrane constructs, the aim was to keep both faces of the lipid bilayer equivalent in lateral area while also retaining phospholipid proportions. All membrane systems discussed herein are under 9000 $Å^2$ in lateral area, but most are approximately 8500 $Å^2$, and all total under 300 total lipids in each bilayer. These 'lipid slab images' were duplicated using periodic boundary conditions; this allows atoms on the exterior of the lateral plane to be treated as surrounded by atoms, despite the absence of an image.[44]

Coulombic interactions were included using the particle mesh Ewald (PME) algorithm[48] with a 10 Å cutoff and van der Waals interactions were calculated with a 9 Å cutoff switching function. The isobaric-isothermic, or NPT, ensemble was applied to sustain a constant number of moles, temperature (310K, with a dampening coefficient of 1 ps^{-1}) and pressure (p = 1.01325 bar, piston period/decay of 200/50 fs) of each system. The SHAKE algorithm was utilized to restrain hydrogen bonding, as well as a 2 fs integration time step; this translated to 0.1 ns per frame of the trajectory. Throughout all simulations, the sodium chloride concentration remained at 0.15 M. Calculations were performed on both Reggio lab and BSBC cluster machines at the University of North Carolina at Greensboro.

Visualization and Analysis Software: VMD,[49] LOOS,[50] & APL@Voro[51]

VMD was utilized for visualization of all membrane systems, as well as for the collection of hydrogen bonding data. Donor-hydrogen-acceptor atom bond angle cutoff was set to 35 °, and the donor-acceptor atom distance was set to 3.5 Å, in accordance with a previous investigation.[35] Herein, only heteroatoms were considered for hydrogen bonding pairs.

Membrane structural data, density distribution plots and order parameters, were collected for each bilayer through the prewritten tools available through LOOS (Lightweight Object Oriented Structure-analysis) software. Density distributions are generated by initially defining specific sets of atoms, such as those defining the phospholipid head-group or phosphate. LOOS then generates 'slices' of the system's z-axis and calculates a density probability at half-angstrom intervals. Order parameters are calculated using the standard S_{CD}, by measuring the angle between carbon-hydrogen bond and the plane perpendicular to the bilayer, and averaging over the trajectory.[52]

Initially, surface area per lipid was calculated in VMD by taking the lateral area, or the x-y plane, of the bilayer system and dividing this value by the number of phospholipids in each leaflet. This method is useful to determine area per lipid of single-component bilayer and for the overall bilayer dimension, but cannot differentiate between specific lipid species in mixtures. Thus, the analysis tool APL@Voro was used for all subsequent systems. This software was developed for a different molecular dynamics method, but is apt to analyze the CHARMM trajectories herein. The algorithm generates polygons, centered by user-defined atom selections; the area of these polygons at a

particular point in the trajectory is the area per lipid, recorded and averaged over time. Phosphorus atoms were used for phospholipids, carboxylate carbons for NAGly, and hydroxyl oxygens for cholesterol.

Membrane Compositions: Bilayers 0-5

In Chapters III-IV, five mixed-membrane compositions that include NAGly are discussed. Table 1 lists the percentage of phospholipids in Bilayers 0-5. Phospholipid species proportions are taken from the characterization of synaptic plasma membranes as well as general considerations of mammalian plasma membranes. Percentages were altered slightly to achieve an equivalent surface area between extracellular and intracellular leaflets, using the area per lipids provided by CHARMM-GUI. All membrane compositions were simulated for more than 200 nanoseconds (ns).

Additional compositions lacking ligands were also constructed and calculated to ensure accuracy of Bilayers 0-5; these compositions are shown in Appendix A. Similar trends in data were obtained between equivalent compositions, thus the discussion herein focuses on membranes including NAGly. Bilayer 0, consisting solely of 1-palmitoyl-2-oleoyl-*sn*-glycero-3-phosphatidylcholine phospholipids and NAGly, is largely excluded from the following discussion. It was calculated at 298 K with an equal amount of sodium and chloride ions, while the heterogeneous membranes, Bilayers 1-5, were calculated at 310 K with additional neutralizing sodium for anionic lipids. The comparison of a pure phosphatidylcholine leaflet properties to heterogeneous ones uses the single-phospholipid extracellular leaflet of the initial mixed composition, Bilayer 1. Bilayer 0 was utilized solely for the comparison of AEA and NAGly hydrogen bonding

patterns in Chapter IV, since Bilayer 0 is more similar to previous AEA studies and thus more applicable for the discussion than the extracellular leaflet of Bilayer 1.

Table 1. Compositions of Bilayers 0-5. PC = phosphatidylcholine, PE = phosphatidylethanolamine, PS = phosphatidylserine, SM = sphingomyelin, PIP2 = phosphatidylinositol-4,5-biphosphate, CHL = cholesterol. Values provided are mole percentages of the total lipid in the bilayer.

Bilayer	Leaflet	PC	PE	SM	PS	PIP2	CHL	PUFAs	NAGly
0	*Extracellular*	90.84%	-	-	-	-	-	-	9.16%
	Cytosolic	90.84%	-	-	-	-	-	-	9.16%
	Total	90.84%	-	-	-	-	-	-	9.16%
1	*Extracellular*	90.84%	-	-	-	-	-	-	9.16%
	Cytosolic	71.64%	-	-	19.40%	-	-	-	8.96%
	Total	81.13%	-	-	9.81%	-	-	-	9.06%
2	*Extracellular*	73.64%	17.05%	-	-	-	-	-	9.30%
	Cytosolic	29.93%	41.61%	-	19.71%	-	-	-	8.76%
	Total	51.13%	29.70%	-	10.15%	-	-	-	9.02%
3	*Extracellular*	64.62%	18.46%	7.69%	-	-	-	-	9.23%
	Cytosolic	25.74%	42.65%	-	19.85%	2.94%	-	-	8.82%
	Total	44.74%	30.83%	-	10.15%	1.50%	-	-	9.02%
4	*Extracellular*	51.47%	19.12%	7.35%	-	-	12.50%	-	9.56%
	Cytosolic	14.79%	41.55%	-	19.72%	2.82%	11.97%	-	9.15%
	Total	32.73%	30.58%	-	10.07%	1.44%	12.23%	-	9.35%
5	*Extracellular*	56.45%	22.58%	8.06%	-	-	12.90%	11.29%	10.48%
	Cytosolic	17.19%	44.53%	-	21.09%	3.13%	14.06%	34.38%	10.16%
	Total	36.51%	33.73%	-	10.71%	1.59%	13.49%	23.02%	10.32%

CHAPTER III

STUDY ONE: PHOSPHOLIPIDS AND CHOLESTEROL

Figures 5A and 5B show the density distributions of Bilayers 1 and 5, omitting NAGly for the discussion of phospholipids and cholesterol herein. Table 2 shows the average structural parameters of major phospholipids in Bilayers 1-5, over four samples totaling 100 ns for each composition. Area per lipid and order parameters were similar among phospholipid species in a corresponding leaflet, but each leaflet was quite distinct.

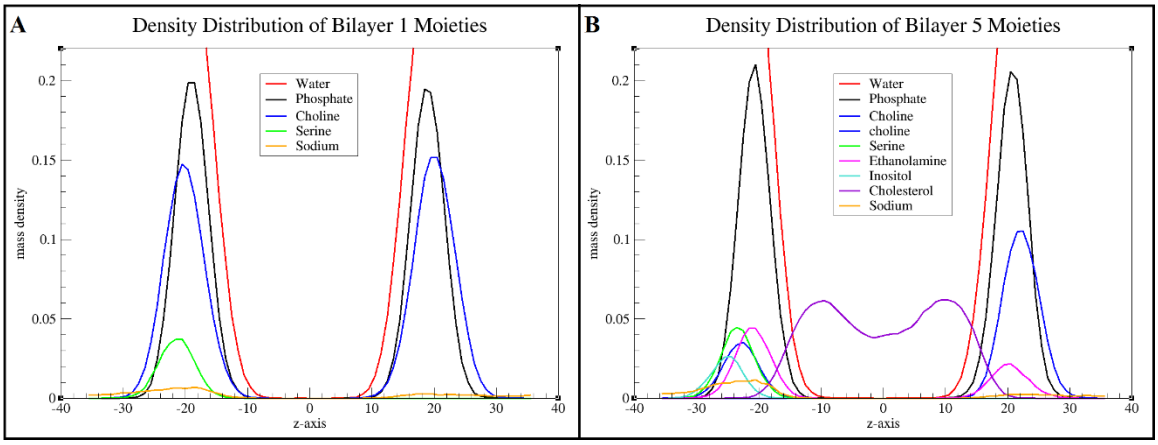

Figure 5. Density Distributions of Bilayers 1 and 5 without NAGly. (A) Density Distribution of Bilayer 1 and (B) Bilayer 5. The z-axis coordinate of zero indicate the center of the bilayer. Negative z-axis coordinates indicate the cytosolic leaflet, while positive coordinates indicate the extracellular leaflet.

Table 2. Average Structural Parameters of Major Phospholipids. PO- = *sn*-1-palmitoyl-*sn*-2-oleoyl-, SD- = *sn*-1-stereoyl-*sn*-2-docosahexaenoyl, DP- = dipalmitoyl. -PC = phosphatidylcholine, -PS = phosphatidylserine, -PE = phosphatidylethanolamine.

		Average Area per Lipid (Å^2)			
Composition	**Leaflet**	**POPC**	**POPE**	**POPS**	-
Bilayer 1	***Extracellular***	65.74	-	-	-
	Cytosolic	65.04	-	62.00	-
Bilayer 2	***Extracellular***	65.61	58.04	-	-
	Cytosolic	63.72	58.28	59.32	-
Bilayer 3	***Extracellular***	64.79	58.80	-	-
	Cytosolic	64.08	58.36	61.16	-
Bilayer 4	***Extracellular***	60.99	54.77	-	-
	Cytosolic	61.30	54.59	54.19	-
		POPC	**SDPE**	**SDPS**	**DPPC**
Bilayer 5	***Extracellular***	61.91	56.51	-	-
	Cytosolic	-	57.12	59.94	61.79
		Average Order of Carbons 2-16 of *sn* -1 chain			
Composition	**Leaflet**	**POPC**	**POPE**	**POPS**	-
Bilayer 1	***Extracellular***	0.144	-	-	-
	Cytosolic	0.154	-	0.161	-
Bilayer 2	***Extracellular***	0.157	0.143	-	-
	Cytosolic	0.180	0.177	0.184	-
Bilayer 3	***Extracellular***	0.158	0.149	-	-
	Cytosolic	0.183	0.174	0.182	-
Bilayer 4	***Extracellular***	0.187	0.186	-	-
	Cytosolic	0.210	0.211	0.217	-
		POPC	**SDPE**	**SDPS**	**DPPC**
Bilayer 5	***Extracellular***	0.189	0.178	-	-
	Cytosolic	-	0.203	0.212	0.213

Phosphatidylcholine

In a phosphatidylcholine bilayer, water molecules can penetrate a membrane, but bulk water does not permeate past phospholipid glycerol oxygens, as seen in previous Reggio molecular dynamics simulations.[35,36] Phosphate density peaks are located approximately 20 Å from the bilayer center, and choline head-groups overlap with phosphates, consistent with a tilted orientation, as shown in Figure 6B, instead of an

upright position in bulk water, as shown in Figure 6A. The tilted orientation of choline reduces the electrostatic repulsion between phosphates, although a dense water network is also present in phosphatidylcholine bilayers.[11]

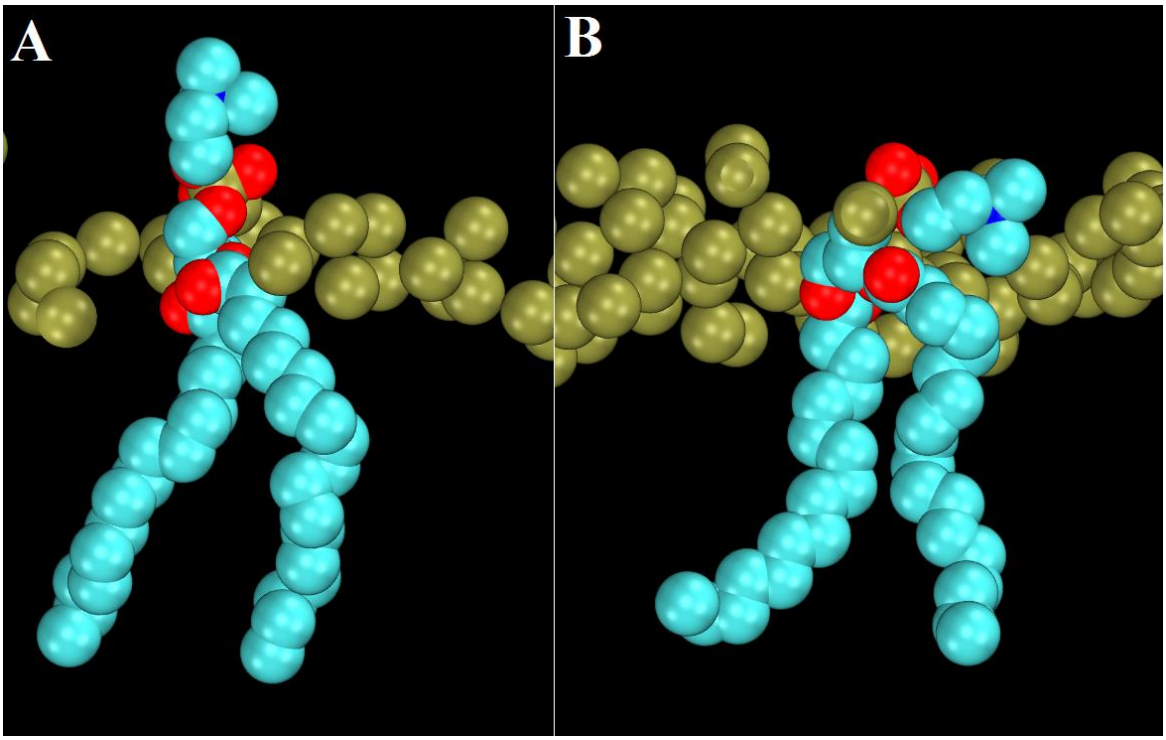

Figure 6. Head-Group Conformations of Phosphatidylcholine. (A) Tilted and (B) upright orientations with respect to the membrane surface. Phosphatidylcholine carbons shown in cyan van der Waals, phosphorus shown in gold spheres, nitrogen shown in blue and oxygens shown in red. Nonpolar hydrogens omitted for clarity.

The area per lipid of phosphatidylcholine in the extracellular leaflet of Bilayer 1 was 65.7 $Å^2$, and the average order along the *sn*-1 chain, or palmitic acid, was 0.144, as shown in Table 2. Both values are in agreement with other simulations[53] and experiments[53,54] conducted at a similar temperature. The area per lipid of phosphatidylcholine in the both leaflets of Bilayer 5 was decreased compared to Bilayer 1

by more than 3 Å^2, and the average order parameter of the *sn*-1 chain was increased by approximately 0.05 in either leaflet. The structural parameters of phosphatidylcholine underwent an enormous change the most from the extracellular leaflet of Bilayer 1. In the Bilayer 5 composition, phosphatidylcholine is a minor percentage of the cytosolic leaflet, but remains the major lipid species of the extracellular leaflet. Order parameters of phosphatidylcholine in Bilayers 1-5 are shown in Figure 7.

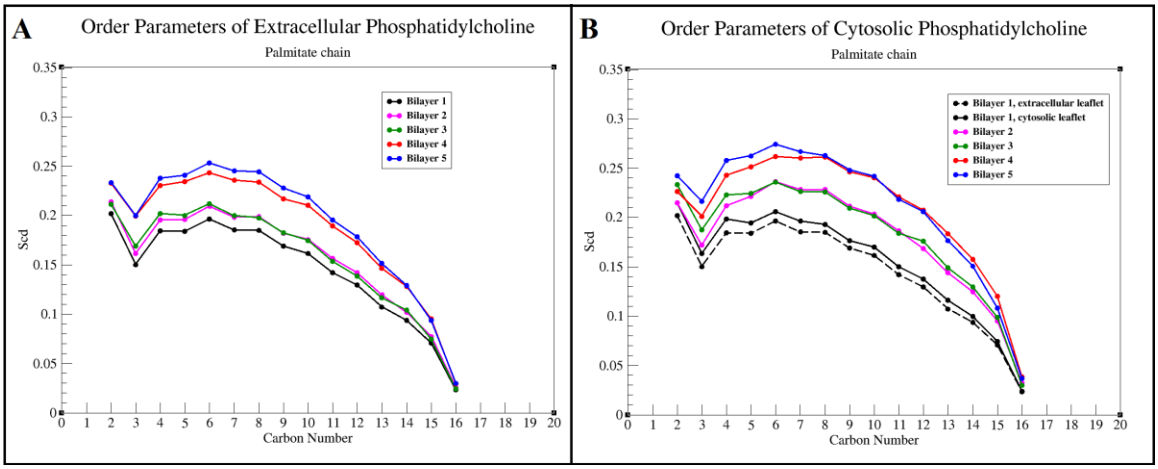

Figures 7. Order Parameters of Phosphatidylcholine in Bilayers 1-5. (A) In the extracellular leaflet and (B) the cytosolic leaflet.

The order parameter of palmitic acid in phosphatidylcholine increased twice, in the cytosolic leaflet when phosphatidylethanolamine was incorporated in Bilayer 2, and when cholesterol was incorporated in Bilayer 4. Cholesterol was anticipated to increase order parameters, but the inclusion of phosphatidylethanolamine was not; it is interesting to note that phosphatidylcholine is a minor lipid of the cytosolic leaflet of all but Bilayer 1, and phosphatidylethanolamines are generally more ordered than phosphatidylcholines.

Phosphatidylcholine order parameters were mostly unchanged between Bilayers 4 and 5, but this species was not selected to be olefinated so as to more accurately mimic a synaptic membrane composition.[7,8]

Phosphatidylserine

The inclusion of phosphatidylserine did not alter structural parameters of phosphatidylcholine in either leaflet, as shown in Table 2. In the cytosolic leaflet of Bilayer 1, phosphatidylserine area per lipid was dissimilar from literature values of pure bilayers.[32] In another all-atom investigation of a two-component membrane, using a similar composition of choline/anionic phospholipids, the average structural parameters of a two-component bilayer were unchanged from a pure phosphatidylcholine leaflet.[53] It is reasonable to conclude as a minor component of the cytosolic leaflet, the bulk phosphatidylcholine skews area per lipid and order parameter values from pure bilayers. When phosphatidylethanolamine was included in the cytosolic leaflet of Bilayer 3, order parameters of the *sn*-1 chain resembled those of simulated pure phosphatidylserine bilayers more closely at 59.3 $Å^2$.[32] Representative order parameters of the *sn*-1 chain of phosphatidylserine in Bilayers 1 through 5 are shown in Figure 8A, with the *sn*-2 chain order parameters shown in Figure 8B. Phosphatidylserine order parameters saw a similar order parameter increases to phosphatidylcholine, in Bilayers 2 and 4. Docosahexaenoic acid was incorporated into the *sn*-2 position of phosphatidylserine in Bilayer 5, as shown in Figure 8B. A decrease in *sn*-1 order was not seen here, as was seen in 100% mixed chain membranes.[23]

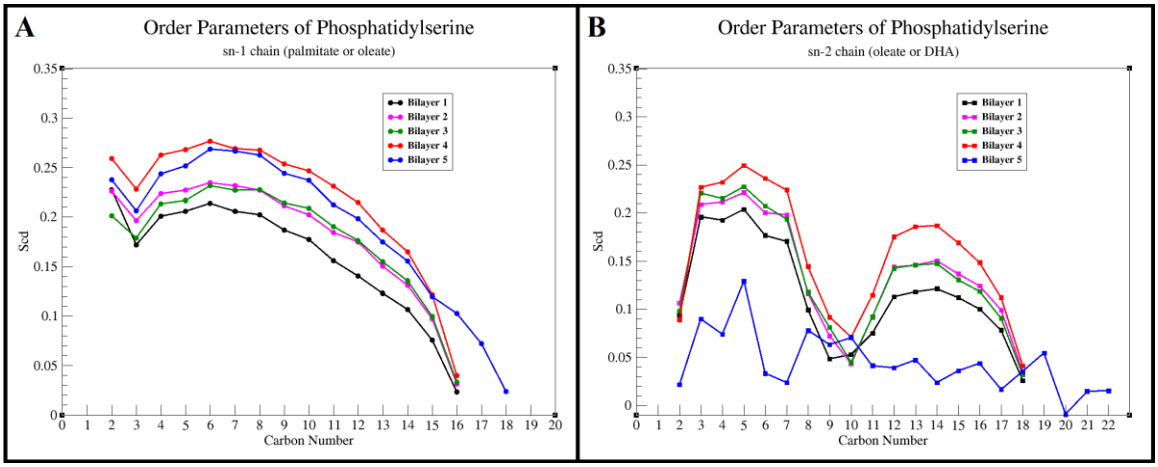

Figure 8. Order Parameters of Phosphatidylserine in Bilayers 1-5. Order of (A) *sn*-1 chains and (B) *sn*-2 chains.

Phosphatidylserine has an overall anionic charge, and thus the CHARMM-GUI algorithm included additional neutralizing sodium ions to the system. While recent advances in the CHARMM36 force field increase the accuracy of phospholipid-sodium interactions, the charged components still have a binding lifetime up to 17.0 ns.[32] In general, sodium[55,56] and calcium[57,58] ions have shown to coordinate phospholipids and reduce electrostatic repulsion, and this was observed in heterogeneous membranes herein. The anionic carboxylate of serine increases the likelihood of clustering around sodium ions, as shown in Figure 9A. Clustering of phosphatidylserine does not have to be coordinated around ions. Since serine has both anionic and cationic groups at physiological pH, clustering of phosphatidylserines has been observed through multiple intermolecular hydrogen bonds,[3,55] similar to Figure 9B. Intramolecular interactions of phosphatidylserine, like the one shown in Figure 9A, promote the head-group to adopt a parallel orientation.[12]

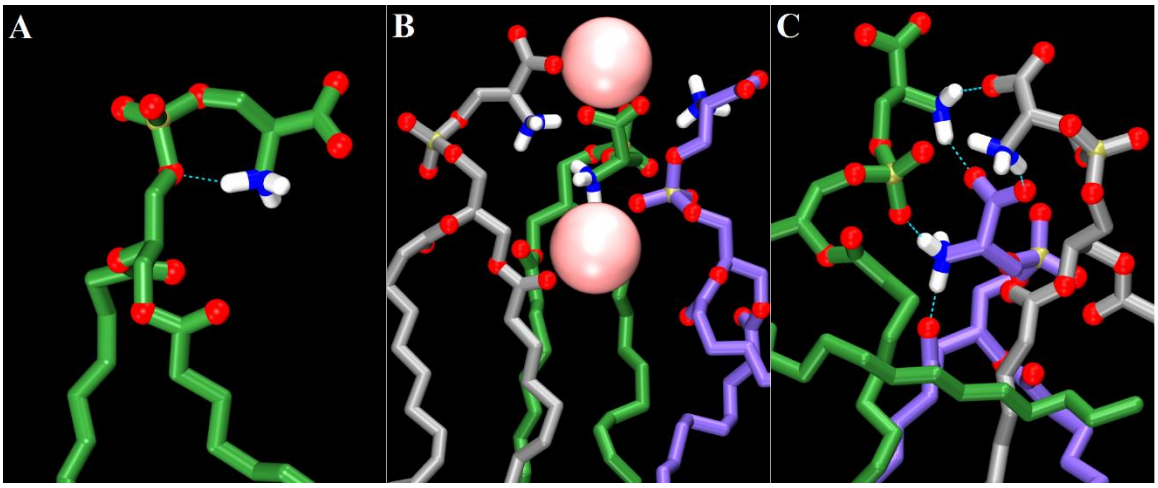

Figure 9. Phosphatidylserine Interactions. (A) An intramolecular hydrogen bond, and clustering of three lipids by (B) sodium ions or (C) hydrogen bond networks. Carbons colored green, violet, or silver to differentiate lipids. Nitrogens colored blue, oxygens colored red, polar hydrogens shown in white, and phosphorus colored gold. Sodium shown in pink spheres and hydrogen bonds shown by cyan dashes. Nonpolar hydrogens omitted for clarity.

Phosphatidylethanolamine

As shown in Table 2, the average area per lipid of phosphatidylethanolamine in either leaflet is approximately 58 $Å^2$, in excellent agreement with other molecular dynamics investigations of pure and mixed phosphatidylethanolamine bilayers.[13,59] In NMR experiments of lipid bilayers composed of choline/serine/ethanolamine lipids, the average order parameter of phosphatidylcholine and phosphatidylserine was increased compared to pure bilayers.[23] In Bilayer 2, a similar increase was observed in palmitate order parameters of cytosolic phosphatidylcholine and phosphatidylserine compared to Bilayer 2. Representative order parameters of phosphatidylethanolamine in Bilayers 2-5 are shown in Figures 10. Phosphatidylethanolamine order parameters saw an increase in order parameters upon cholesterol inclusion in Bilayer 4, and similarly to

phosphatidylserine, when docosahexaenoic acid was incorporated into the *sn*-2 position in Bilayer 5, the average *sn*-1 order was not changed.

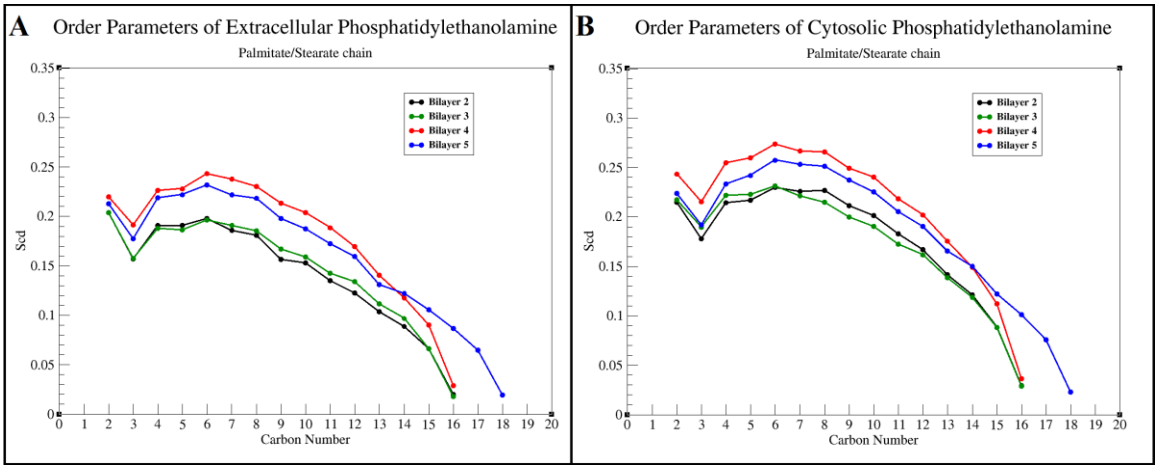

Figure 10. Order Parameters of Phosphatidylethanolamine in Bilayers 2-5. (A) In the extracellular leaflet and (B) the cytosolic leaflet. The average order parameters of the *sn*-2 chain (not shown) were similar to phosphatidylserine.

Pure phosphatidylethanolamine bilayers have unique phase behaviors attributed to the formation of strong hydrogen bonding networks,[4,13,60] similar to Figures 11A and 11B. These matrix of tight bonding prompts tighter lateral packing of the bilayer and a smaller area per lipid requirement compared to choline or serine. Additionally, ethanolamine interacts with water less than choline due the formation of strong phosphate-amine hydrogen bonds not present in phosphatidylcholine bilayers.[11,59,61]

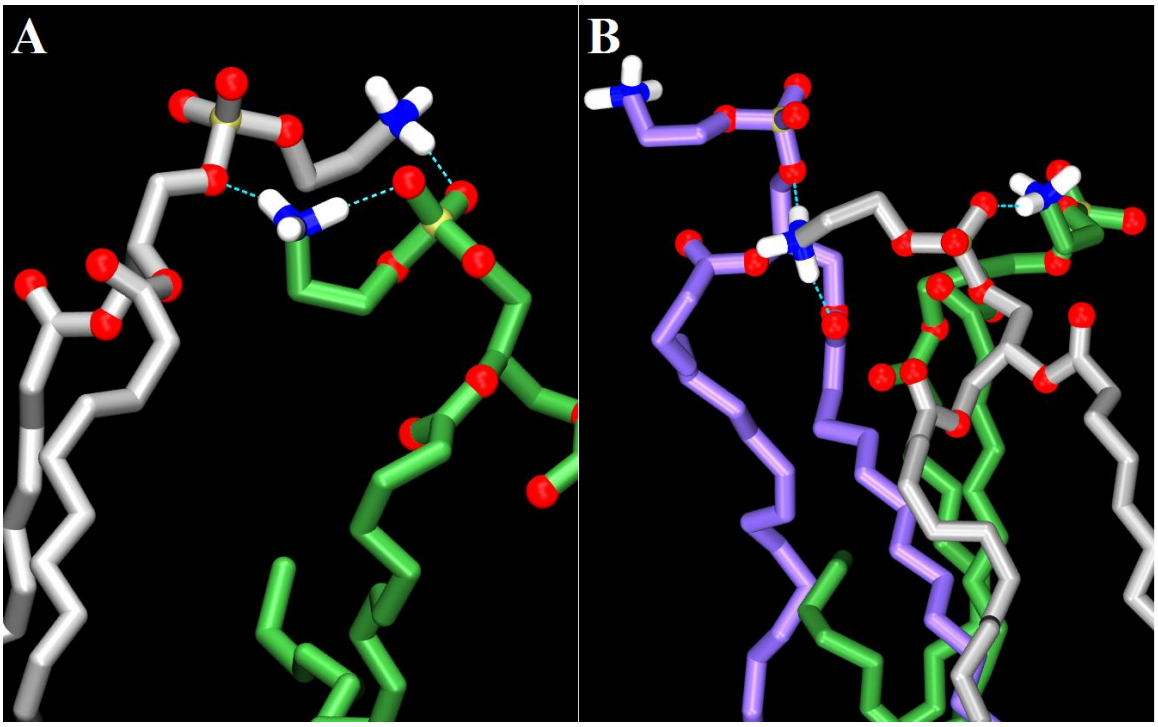

Figure 11. Phosphatidylethanolamine Hydrogen Bond Networks. Two examples of hydrogen bonding between (A) two and (B) three lipids. Carbons colored green, violet, or silver to differentiate lipids. Nitrogens colored blue, oxygens colored red, polar hydrogens colored white, and phosphorus colored gold. Hydrogen bonds shown by cyan dashes. Nonpolar hydrogens omitted for clarity.

Other Phospholipids

The addition of sphingomyelin to the extracellular leaflet in Bilayer 3 did not have an effect on structural properties of major phospholipids. In the extracellular leaflet of Bilayers 3-5, sphingomyelin and phosphatidylcholine are very similar in order parameters, despite the different shapes of the curve in Figure 12, due to a sphingosine core instead of a glycerol core of the phospholipid.

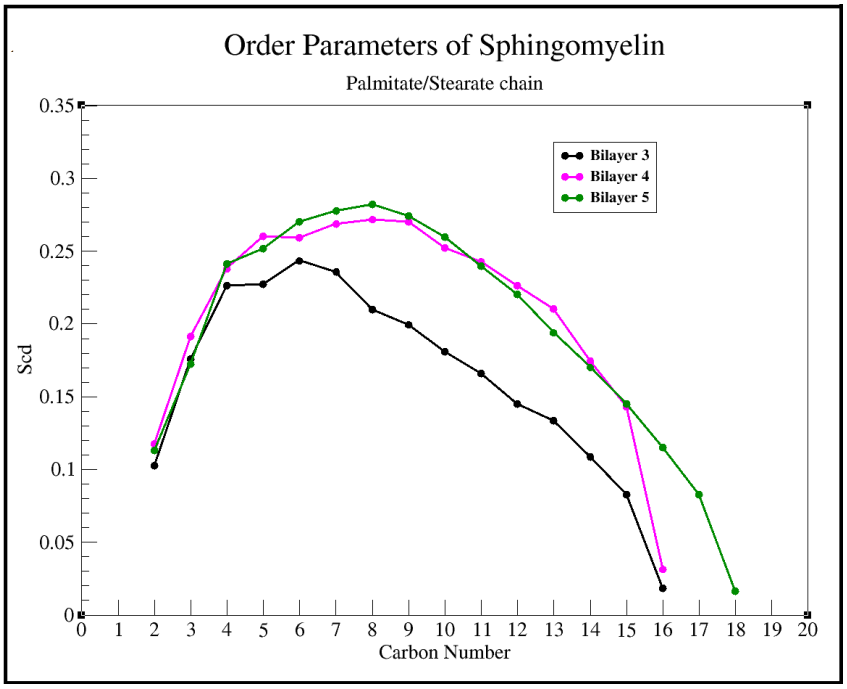

Figure 12. Order Parameters of Sphingomyelin in Bilayers 3-5.

Previous studies of an non-phosphorylated inositol lysophopholipid[35] and phosphoinositides[62] show that the sugar ring is tilted parallel to the bilayer surface and hydrogen bonds with surrounding phospholipids. In Bilayer 3-5, phosphatidylinositol-4,5-biphosphate hydrogen bonds with surrounding phospholipids, as shown in Figure 13, to stabilize this tilted conformation. The additional anionic charge of inositol-phosphate phospholipids added significantly more neutralizing sodium to Bilayers 3-5 compared to previous compositions. Sodium ions were gathered around the inositol-phosphates and bridged multiple anionic moieties, similar to phosphatidylserine.

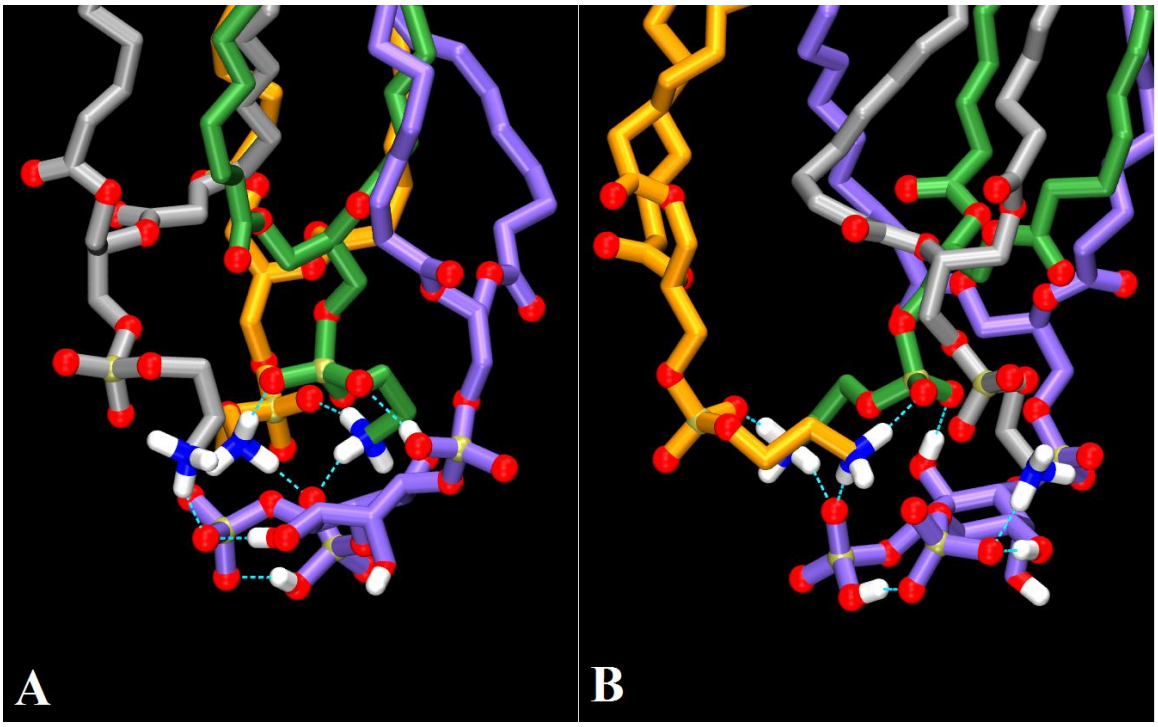

Figure 13. Phophatidylinositol-4,5-biphosphate Hydrogen Bonding Capability. (A) and (B) show different angles of a hydrogen bond network, in cyan dashes, between a single phophosphatidylinositol-4,5-biphosphate, carbons shown in purple, and several phosphatidylethanolamines, carbons in green, orange, or silver to differentiate lipids. Nitrogen shown in blue, phosphorus shown in gold, oxygen in red, and polar hydrogens in white. Nonpolar hydrogens omitted for clarity.

Cholesterol

Structural Changes. Cholesterol was included in Bilayer 4 prior to the olefination of phospholipids in Bilayer 5 to compare effects on membrane structure in contrasting hydrophobic surroundings. Cholesterol is known to pack well with saturated fatty acids, increasing phospholipid order parameters and condensing area per lipid. Cholesterol inclusion in Bilayer 4 increased the average order parameter of palmitate in all species by approximately 0.03 from Bilayer 3, and decreased the average area per lipid by as much

as 4 $Å^2$ for phosphatidylcholine and phosphatidylethanolamine. Additionally, cholesterol thickens the membrane bilayer,[14] as shown in Figure 14 by the widening of the density distribution from the bilayer center.

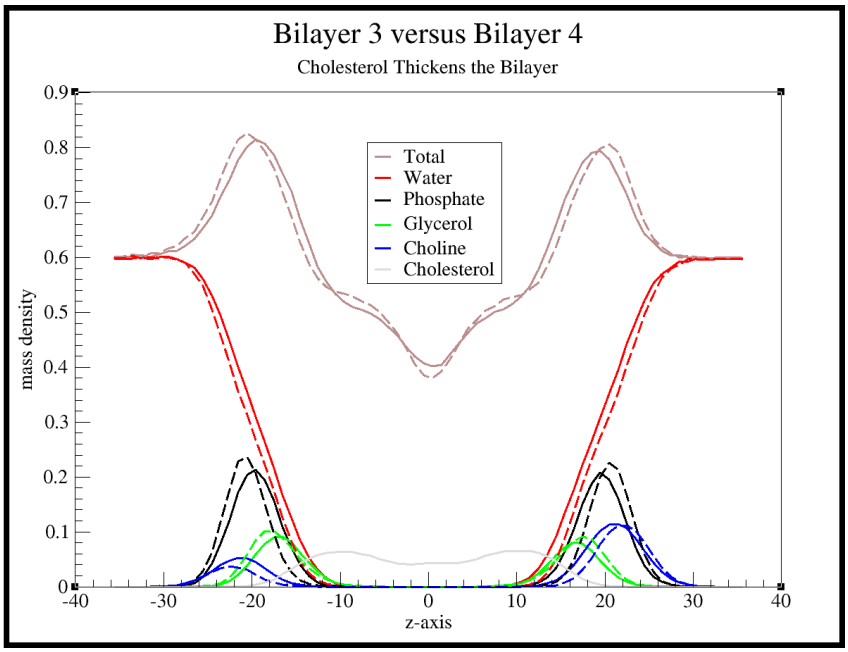

Figure 14. Cholesterol Thickens the Bilayer. Density distributions of components of Bilayers 3 and 4. Solid lines shown Bilayer 3, dashed line for Bilayer 4. The z-axis coordinate of zero indicate the center of the bilayer. Negative z-axis coordinates indicate the cytosolic leaflet, while positive coordinates indicate the extracellular leaflet.

Cholesterol-Phospholipid Preferences. Huster et al. estimated the strength of cholesterol interaction with a specific phospholipid species on the change in the average order parameters between a bilayer including or lacking cholesterol.[23] They found that when mixtures of ethanolamine/serine/choline phospholipids contained monounsaturated *sn*-2 chains, cholesterol preferred phosphatidylethanolamine greatest and phosphatidylserine the least. This preference is reversed in a similar mixture of

phospholipids containing polyunsaturated *sn*-2 chains and more pronounced than the monounsaturated mixture. Huster et al., 1998 also observed that phosphatidylserine had little change in order parameter, and thus little interaction with cholesterol in a ternary mixture. Table 3 shows the changes in average order parameter of major phospholipids in Bilayers 3 and 4**.**

Table 3. Changes in Order Parameters between Bilayers 3 and 4. Order parameter change was measured using the average values of the palmitate chains of major phospholipids in Table 2. POPS = phosphatidylserine, POPE = phosphatidylethanolamine, POPC = phosphatidylcholine. Positive values indicate an increase upon the addition of cholesterol.

		Change in Average Order Parameter of *sn* -1 chain			
Composition	**Leaflet**	**POPC**	**POPE**	**POPS**	-
Bilayer 4-3	***Extracelluar***	0.029	0.036	-	-
	Cytosolic	0.026	0.037	0.034	-

The comparison between the cytosolic leaflets of Bilayer 3 and 4 to monounsaturated mixtures, there is a larger increase in order for ethanolamine compared to choline, thus cholesterol prefers ethanolamine over choline monounsaturated phospholipids, consistent with Huster et al. However, in contrast to those NMR experiments, phosphatidylserine has the greatest change in order, suggesting it is preferred most by cholesterol. This is likely due to the increased concentration of phosphatidylserine in the cytosolic leaflet of all Bilayer compositions; the NMR experiments were performed with half the amount. However, recent experimental studies have shown that phosphatidylserine is necessary to maintain cholesterol in the cytosolic leaflet,[15] so cholesterol preferring phosphatidylserine is plausible.

Cholesterol Flip-Flop. Cholesterol was observed in both positions in Bilayer 5, but it did not tilt as freely in Bilayer 4. The reorientation of cholesterol to the methyl region of the bilayer can lead to a cholesterol flip-flop, where cholesterol transitions from an upright position in one leaflet to the same canonical position in the opposing leaflet. Cholesterol flip-flops have been observed in a variety of molecular dynamics simulations, even those with fully saturated bilayers. Herein, there were only two events of full cholesterol flip-flop observed, both in Bilayer 5, however several molecules relocated to the center of the bilayer and returned to the original upright position in the final membrane composition without ligands.

Canonical Mechanism. Molecular dynamics simulations by Kucerka et al. 2008[26] showed that cholesterol flip-flop was initially induced by hydrogen bonding between a cholesterol hydroxyl and either surrounding water or phospholipid. These interactions guide the steroid to tilt, and thus easily transitions the hydroxyl into the acyl region of the bilayer.[26] In a ligand-included equivalent to Bilayer 5, an extracellular cholesterol flip-flopped by a similar mechanism, shown in Figure 15.

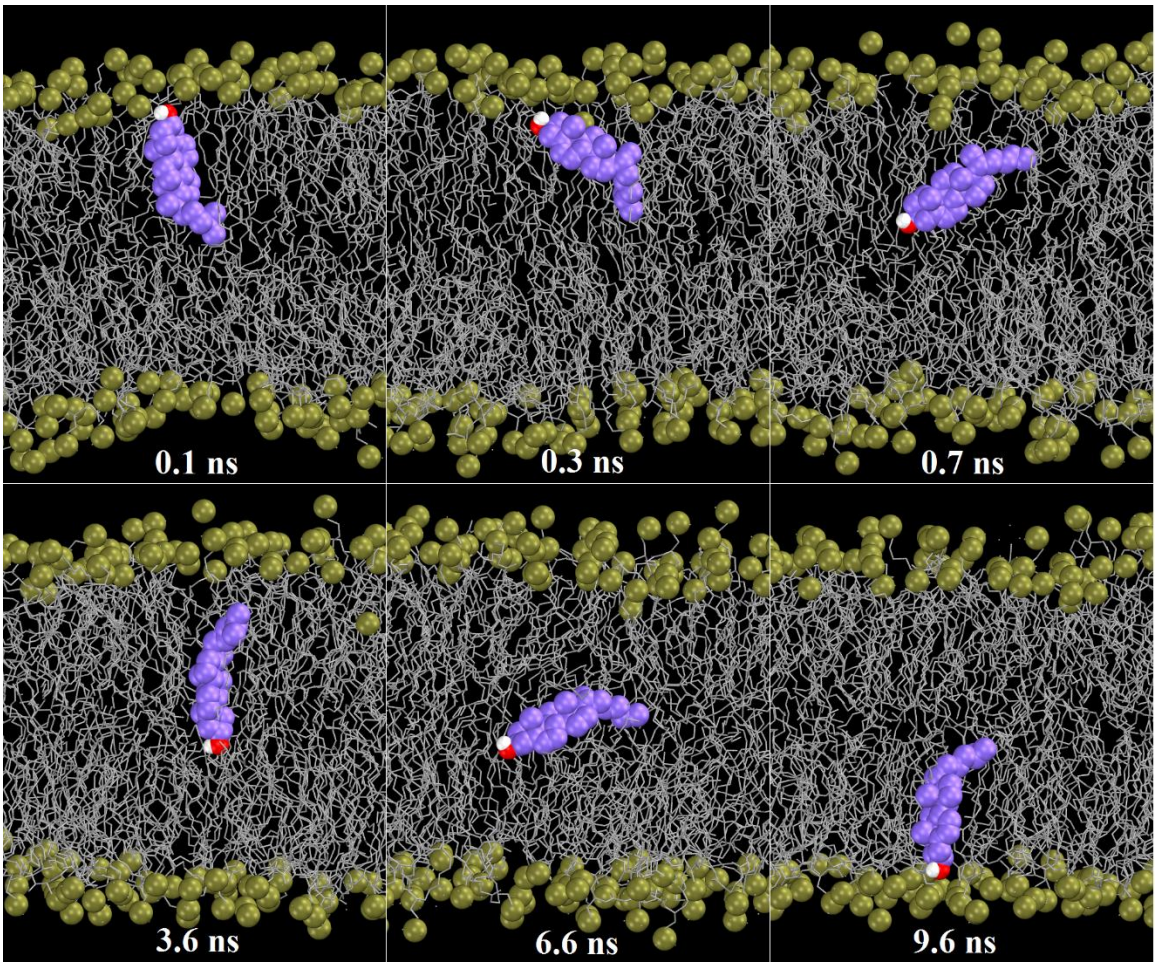

Figure 15. Canonical Cholesterol Flip-flop. Oxygen shown in red, hydrogen in white, and carbons shown in violet. Acyl chains shown in silver sticks. Phosphorus shown in gold spheres. Nonpolar hydrogens omitted for clarity.

The initial tilt and dive of the steroid was fast and dramatic, but in contrast to Kucerka et al. 2008,[26] a persistent water molecule did not assist in the transition of the hydroxyl away from the water interface. Instead, the initial tilting of the steroid appears to be due to water pocket formed by a large spacing in surrounding extracellular phosphates exposing the hydrophobic steroid to water; the transition appears to be a mechanism to avoid water interactions. After residing in the methyl region of the bilayer

for more than 5 ns, hydrogen bonding with a cluster of cytosolic ligands tilted the steroid towards cytosolic phosphates. This event is discussed further in Chapter IV.

Non-canonical Mechanism. In addition to a canonical cholesterol transition, another contrasting mechanism of flip-flop occurred was observed. Previously, hydrogen bonds formed and initiated a tilt in the steroid, but in the alternate flip-flop event a cholesterol molecule transitioned to the opposing leaflet in an upside-down-upright orientation, prior to the reorientation of the hydroxyl towards the opposing leaflet, as shown in Figure 16.

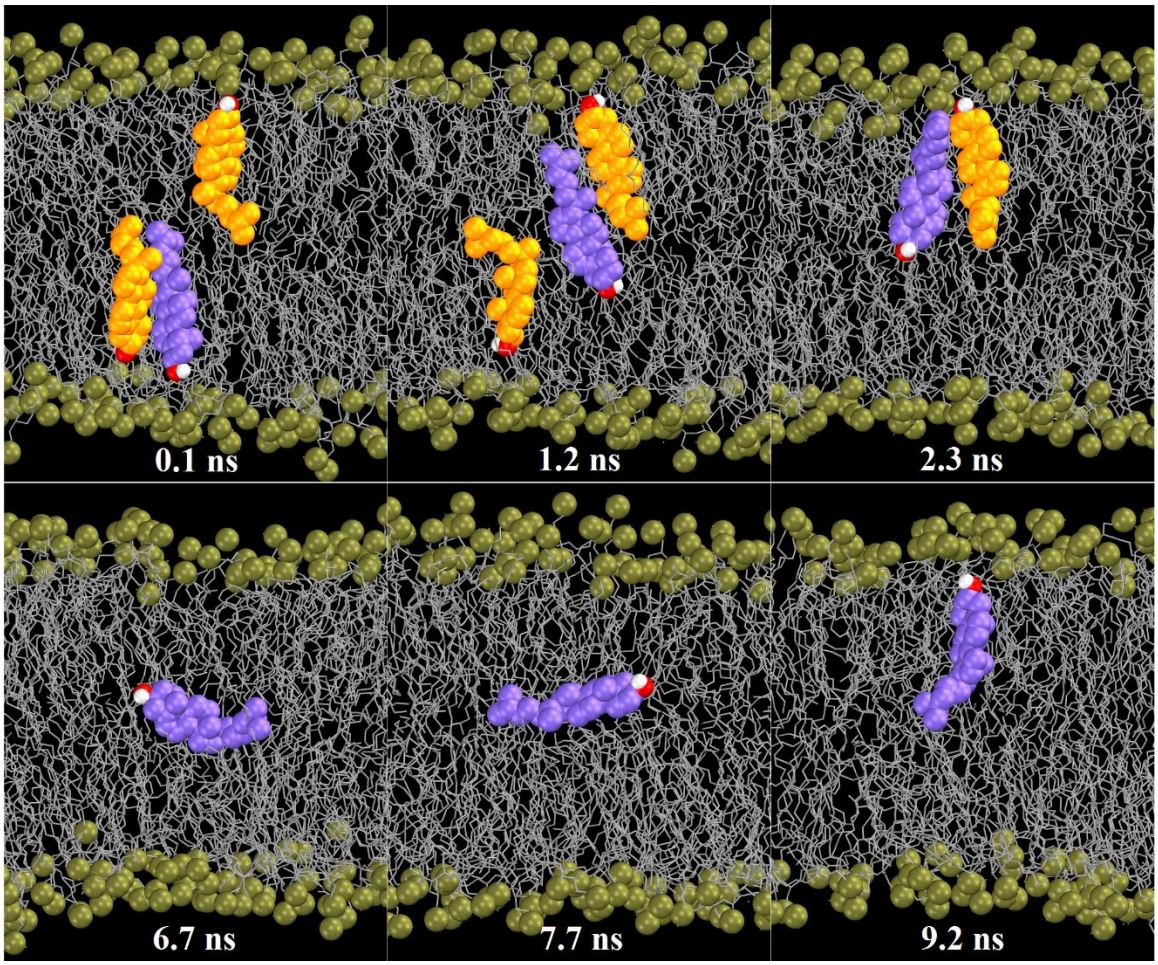

Figure 16. Non-canonical Cholesterol Flip-flop. Oxygen shown in red, hydrogen in white. The cholesterol of interest has carbons shown in violet, accessory cholesterol carbons are shown in orange. Phosphorus represented by gold spheres. Acyl chains shown in silver sticks. Nonpolar hydrogens omitted for clarity.

Rather than avoiding water, like in the previous canonical example, the transitioning cholesterol appeared to use another cholesterol to slide into the opposing leaflet rather than a reorientation and dive seen previously. The initial transition with accessory cholesterols was slower than the canonical mechanism, but after aligning horizontally in the methyl region of the bilayer the hydroxyl reoriented towards the

extracellular phosphates in an upright position. Although this flip-flop occurred in a bilayer which included ligands not discussed in Chapter III, a similar flip-flop mechanism has been observed in a pure phospholipid bilayer. Direct clustering of cholesterol is unfavorable for the membrane structure, and it was determined that this mechanism is less costly in free energy than a canonical mechanism.[28]

Summary & Future Directions

Structural properties of a given bilayer was able to be tracked though the diversification of phospholipid components. In the Bilayer 5 composition, there are five phospholipid species, as well as cholesterol and polyunsaturated fatty acids. Both species have stronger hydrogen bonding potential than choline and consequently pack tightly at the water interface, reflected in smaller area per lipid and increased average order. Incorporation of cholesterol in the bilayer, as well as polyunsaturated fatty acids into serine/ethanolamine/inositol phospholipids, produced expected changes in both order and area per lipid. Heterogeneous bilayer compositions contain fluctuating clusters of phospholipids bound by intermolecular hydrogen bonding and ion coordination, and well as interleaflet transition of cholesterols.

Future membrane investigations are effectively limitless. The model itself can be more refined to be more biologically accurate by including glycolipids, and increasing the concentration of cholesterol.[7,8] Further validation of the results herein will be executed by repeating bilayers with identical compositions and different starting configurations, to analyze the influence of starting structure on phospholipid clustering.

CHAPTER IV

STUDY TWO: N-ARACHIDONOYLGLYCINE

Structural Properties of NAGly in Mixed Bilayers

A density distribution of Bilayers 1 and 5, including NAGly, is shown in Figure 17, and Table 4 lists the structural data for NAGly in Bilayers 1-5.

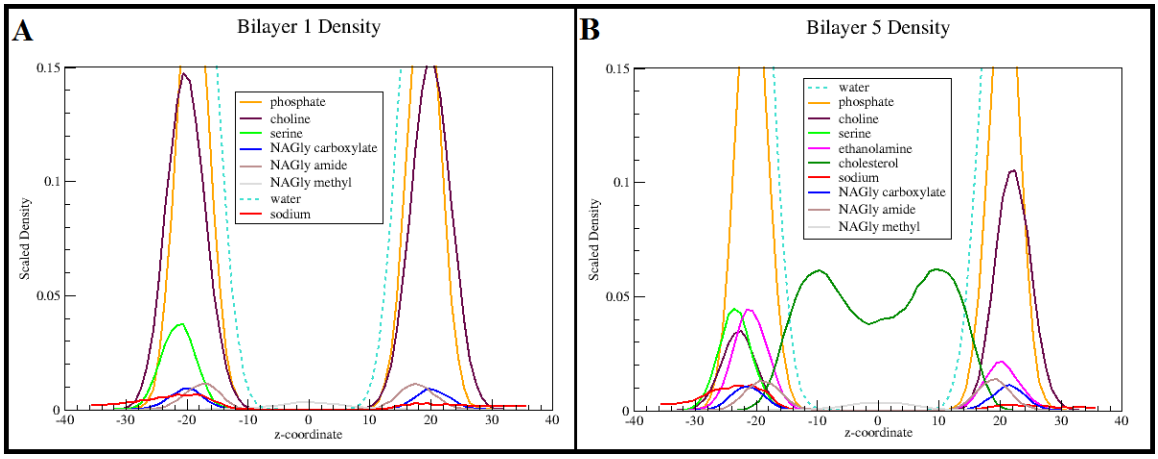

Figure 17. Density Distributions of Bilayers 1 and 5 with NAGly. (A) Bilayer 1 and (B) Bilayer 5. The z-axis coordinate of zero indicate the center of the bilayer. Negative z-axis coordinates indicate the cytosolic leaflet, while positive coordinates indicate the extracellular leaflet.

Table 4. Average Structural Data of NAGly. Area per lipid in Angstroms^2, order parameters shown as an average over the arachidonic acid chain of NAGly.

Composition	Leaflet	AREA	OP
Bilayer 1	***Extracellular***	57.511	0.0552
	Cytosolic	54.779	0.0594
Bilayer 2	***Extracellular***	53.806	0.0582
	Cytosolic	51.614	0.0655
Bilayer 3	***Extracellular***	55.193	0.0583
	Cytosolic	51.812	0.0615
Bilayer 4	***Extracellular***	49.769	0.0671
	Cytosolic	48.839	0.0717
Bilayer 5	***Extracellular***	50.992	0.0645
	Cytosolic	50.455	0.0690

In relation to phosphates, the NAGly carboxylate position is not skewed on average in Bilayers 1-5. In the extracellular leaflet of Bilayer 1, NAGly had an average area per lipid of 57.5 Å^2, and an average order parameter of 0.055. In Bilayer 5, NAGly area per lipid decreased to less than 51 Å^2 in both leaflets. The addition of either phosphatidylserine or phosphatidylethanolamine to the membrane decreased the average area of ligands, compared with the phosphatidylcholine extracellular leaflet. This in in agreement with a lateral packing of serine and ethanolamine lipids.[12] The incorporation of phosphatidylinositol in Bilayer 3 did not have an effect on NAGly area in the cytosolic leaflet, but sphingomyelin in the extracellular leaflet increased the average ligand area slightly. Cholesterol in Bilayer 4 prompted a decrease of almost 5.5 Å^2 in extracellular ligand area per lipid, but cytosolic NAGly only decreased by only 3 Å^2. The olefination of phosphatidylethanolamine and phosphatidylserine in the extracellular and cytosolic leaflet of Bilayer 5 reversed the condensing effect of cholesterol by 1.2 Å^2 and 1.6 Å^2.

Compared to the extracellular leaflet of Bilayer 1, the average area per lipid of NAGly in both leaflets of Bilayer 5 was reduced by 10 % from the pure phosphatidylcholine leaflet of Bilayer 1. Compared to the single-phospholipid leaflet the average order parameter of NAGly was increased, but the arachidonic acid chain is still highly mobile.

NAGly & AEA Hydrogen Bonding in Phosphatidylcholine

The hydrogen bonding patterns of NAGly in Bilayer 0 was compared to those of a structurally similar endocannabinoid, AEA, from previous Reggio investigations.[35] Both NAGly and AEA have of polyunsaturated arachidonic acid scaffold, however NAGly possesses a carboxylate in place of the hydroxyl in AEA.

This small change has great effects the position of the ligand in the bilayer, as shown between Figures 18A and 18B. The NAGly carboxylate is positioned farther from the bilayer center by more than 4 Å, and the charged carboxylate forms hydrogen bonds with water over 96 % of a given sample herein, regardless of membrane composition, as shown in Table 5 and Table 7. In contrast, the neutral hydroxyl of AEA sits deeper in the membrane and hydrogen bonds with water only 86 % of a trajectory sample.[35] However, the amide bond is hydrated similarly between the two ligands, likely due to the preference to form hydrogen bonds with phosphate and glycerol oxygens over water.

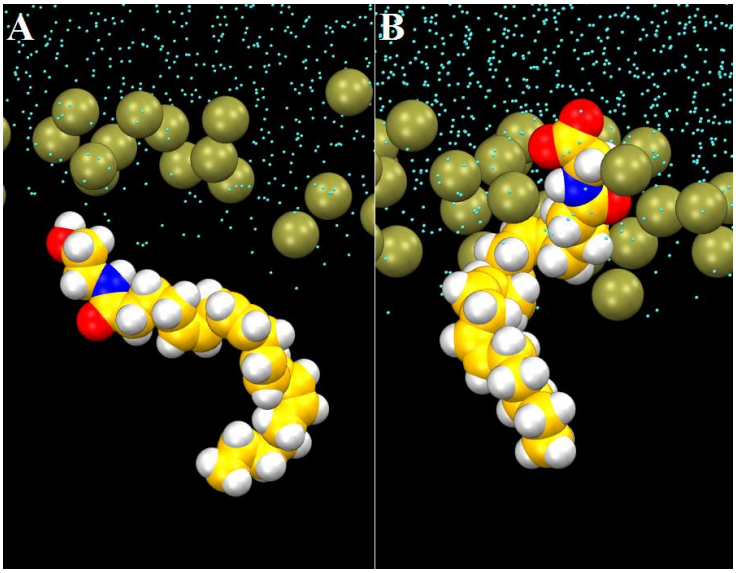

Figure 18. Ligands Positioned in the Bilayer. The position of (A) AEA and (B) NAGly in a phosphatidylcholine bilayer. Water oxygens shown in small cyan spheres, and phosphorus in brown spheres. Ligand carbons colored yellow, nitrogen shown in blue, oxygen in red, and hydrogens in white.

Table 5. Hydrogen Bonding Lifetimes of AEA & NAGly. Listed as a percentage of a 25 ns sample in a given Bilayer trajectory. AEA hydrogen bonding patterns taken from Kotsikorou et al., 2011.[35]

AEA Hydrogen Bonding Lifetimes in Pure POPC				
PC * AEA Pair	Phosphate * NH	Glycerol * NH	Phosphate * OH	Glycerol * OH
% (Pure PC)	3.5	16.6	26.5	6.2
Water * AEA Pair	* OH	* NH	* C=O	
%	86.0	41.0	60.0	
NAGly Hydrogen Bonding				
PC * NAGly Pair	Phosphate * NH	Glycerol * NH	-	-
% (Bilayer 0)	21.38	5.23	-	-
% (Bilayer 5 Extracellular)	13.78	3.55	-	-
% (Bilayer 5 Cytosolic)	11.31	1.52	-	-
Water * NAGly Pair	* COO	* NH	* C=O	-
% (Bilayer 0)	99.02	49.47	76.01	-
% (Bilayer 5 Extracellular)	98.17	48.51	69.70	-
% (Bilayer 5 Cytosolic)	97.28	45.14	68.42	-

Since the choline moiety is excluded from hydrogen bonding analysis herein, the only bonding pairs in Bilayer 0 were between the NAGly amide proton and phospholipid phosphate/glycerol oxygens, examples shown in Figure 19.

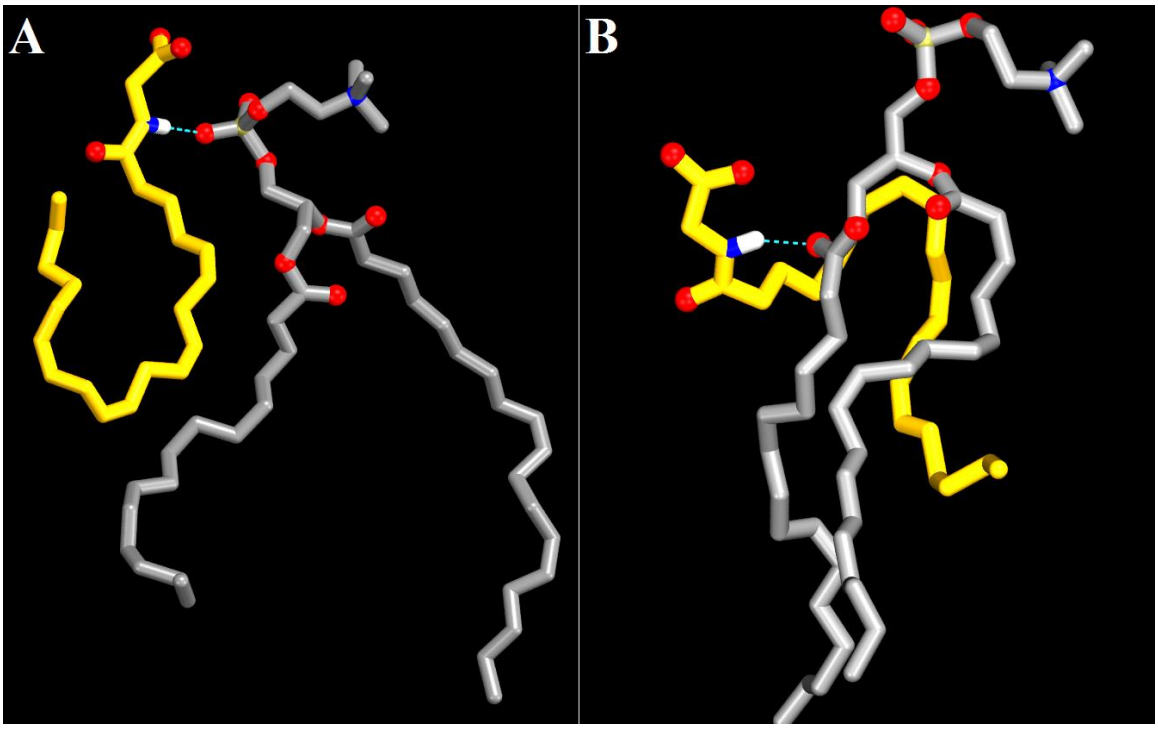

Figure 19. NAGly and Phosphatidylcholine Interactions. NAGly, carbons shown in yellow, forming a hydrogen bond, shown in cyan dashes, with either (A) phosphate or (B) glycerol oxygens of phosphatidylcholine, carbons shown in silver. Nitrogen shown in blue, oxygen in red, phosphorus in gold, and amide proton in white. Nonpolar hydrogens omitted for clarity.

NAGly forms hydrogen bonds with phosphate and glycerol oxygens of phosphatidylcholine for 21 % and 5 % of a 25.0 ns trajectory sample in Bilayer 0, as shown in Table 5. Both interaction lifetimes are in agreement with the of the hydroxyl of AEA rather than the amide.[35,36] The primary hydrogen bond acceptor in a

phosphatidylcholine membrane is the anionic phosphate oxygens, and AEA has two donor protons competing for interactions here. The hydroxyl is positioned closer and thus forms hydrogen bonds more often with phosphate oxygens than the amide proton, which interacts with glycerol oxygens more often in a trajectory sample.[35,36] In contrast, the carboxylate of NAGly is deprotonated and there is no competition for the amide proton to interact with either moiety of phosphatidylcholine. Additionally, since NAGly sits higher in the membrane, its amide is positioned closer to surrounding phosphates. Overall, the amide proton hydrogen bonds with phosphatidylcholine phosphate oxygens significantly longer than the same moiety of AEA.

NAGly Hydrogen Bonding in Mixed Membranes

Hydrogen bonding lifetimes of specific interaction pairs for NAGly and sphingomyelin, phosphatidylcholine, phophatidylserine or phosphatidylethanolamine lipids in Bilayers 1-5 over 100 ns are shown in Table 6, and Table 7 for water. Table 6 is an average over four 25 ns samples, the details of which are presented in Appendix B. Table 8 lists the number of NAGly in a 25.0 ns sample that engaged with a particular lipid species for more than 1.0 ns.

Table 6. Hydrogen Bonding Lifetimes of NAGly with Phospholipids. PO4 = phosphate, O—C=O = glycerol oxygens, NH3 = primary amine, C=O = ligand amide carbonyl, COO = carboxylate, NH = ligand amide proton or sphingomyelin, OH = sphingomyelin alcohol. Lifetime values are a percentages of a 25 ns sample trajectory. An asterisk indicates a phospholipid-ligand bonding pair.

Average NAGly Hydrogen Bonding Lifetimes with Phospholipids						
PL-NAGly	**Leaflet**	**Bilayer 1**	**Bilayer 2**	**Bilayer 3**	**Bilayer 4**	**Bilayer 5**
PL = Phosphatidylcholine						
PO4 * NH	***Extracellular***	23.05	16.79	12.22	13.84	13.78
	Cytosolic	18.38	11.96	10.83	8.43	11.31
O--C=O * NH	***Extracellular***	3.85	3.63	3.65	3.60	3.55
	Cytosolic	3.39	1.63	2.10	0.79	1.52
PL = Phosphatidylethanolamine						
PO4 * NH	***Extracellular***	-	14.29	8.68	10.49	12.04
	Cytosolic	-	16.01	10.23	14.94	16.14
O--C=O * NH	***Extracellular***	-	1.46	1.68	1.69	1.73
	Cytosolic	-	2.48	3.22	2.46	2.41
NH3 * COO	***Extracellular***	-	38.12	27.70	35.08	42.05
	Cytosolic	-	43.58	39.79	43.13	49.59
NH3 * C=O	***Extracellular***	-	3.07	2.32	2.18	2.92
	Cytosolic	-	3.22	3.09	2.97	2.80
PL = Phosphatidylserine						
PO4 * NH	***Cytosolic***	15.54	5.40	7.53	8.59	7.44
O--C=O * NH	***Cytosolic***	2.55	0.97	2.26	3.13	4.21
NH3 * COO	***Cytosolic***	35.07	18.85	36.91	33.27	24.59
NH3 * C=O	***Cytosolic***	1.29	1.52	3.49	1.09	0.69
COO * NH	***Cytosolic***	0.47	0.82	0.93	1.36	0.44
PL = Sphingomyelin						
PO4 * NH	***Extracellular***	-	-	5.70	3.88	7.77
OH * NH	***Extracellular***	-	-	2.60	0.13	0.40
NH * C=O	***Extracellular***	-	-	5.85	8.08	13.32

Table 7. Hydrogen Bonding Lifetimes of NAGly with Water. COO = carboxylate, NH = amide proton, C=O = amide carbonyl. Lifetime values are a percentage of a 25 ns sample trajectory. An asterisk indicates a phospholipid-ligand bonding pair.

		Average Hydrogen Bonding Lifetimes with Water over 100 ns					
NAGly	**Leaflet**	**Bilayer 1**	**Bilayer 2**	**Bilayer 3**	**Bilayer 4**	**Bilayer 5**	**Average**
*** COO**	***Extracellular***	96.83	98.02	96.63	96.20	98.17	97.17
	Cytosolic	97.87	97.29	96.27	96.99	97.28	97.14
*** NH**	***Extracellular***	46.13	47.39	46.67	45.97	48.51	46.93
	Cytosolic	45.47	44.14	46.42	42.20	45.14	44.67
*** C=O**	***Extracellular***	70.00	72.03	70.10	67.07	69.70	69.78
	Cytosolic	71.09	69.02	63.38	67.69	68.42	67.92

Table 8. Number of NAGly Interacting with a Phospholipid. Only ligands that interacted for more than 1.0 ns of a 25.0 ns trajectory sample are considered.

Average Number of NAGly Interacting with a Phospholipid					
Composition	**Leaflet**	**PC**	**PE**	**PS**	**SM**
Bilayer 1	***Extracellular***	12.00	-	-	-
	Cytosolic	10.00	-	8.25	-
Bilayer 2	***Extracellular***	11.00	9.75	-	-
	Cytosolic	6.25	12.00	8.00	-
Bilayer 3	***Extracellular***	10.25	10.50	-	2.50
	Cytosolic	4.25	13.00	6.50	-
Bilayer 4	***Extracellular***	11.00	13.00	-	2.00
	Cytosolic	3.50	13.00	11.50	-
Bilayer 5	***Extracellular***	11.25	13.00	-	1.75
	Cytosolic	3.00	13.00	10.00	-

Phosphatidylcholine. As shown in Table 6 the hydrogen bonding lifetimes of NAGly with phosphatidylcholine in Bilayer 1 decreased by almost 5 % upon the addition of phosphatidylserine to the cytosolic leaflet, compared to the extracellular leaflet. As shown in Table 8 all but 2-3 cytosolic ligands forming hydrogen bonds with phosphatidylcholine in a given sample. Phosphatidylethanolamine in Bilayer 2 decreased the phosphate-amide interaction lifetimes with phosphatidylcholine in both leaflets, and

the extracellular phosphate-amide hydrogen bonding further decreased with sphingomyelin in Bilayer 3. Almost all extracellular NAGly still interacted with phosphatidylcholine in Bilayer 2 and 3, but only approximately five of twelve cytosolic ligands interacted with phosphatidylcholine in Bilayers 2 and 3. Cholesterol in Bilayer 4 decreased phosphate and glycerol interactions in the cytosolic leaflet, but not in the extracellular leaflet. This decrease in lifetime is reversed in Bilayer 5, but less than five of thirteen cytosolic ligands interacted with phosphatidylcholine in a 25.0 ns sample in contrast to the extracellular leaflet. This suggests that while cytosolic ligands of Bilayer 5 are less likely to interact with phosphatidylcholine, the average interaction time is not shortened. Comparatively, extracellular ligands in Bilayer 5 are just as likely to interact with phosphatidylcholine, but on average and individual ligand interacts for less time.

Phosphatidylserine. More than half of all ligands in a cytosolic engaged in amine-carboxylate interactions with phosphatidylserine; this interaction is present on average for a third of a 25.0 ns sample in Bilayer 1-5, as shown in Table 6. Phosphate-amide interactions were present over 15 % of Bilayer 1 but decreased by 10 % in Bilayer 2, similar to phosphatidylcholine. The addition of cholesterol in Bilayer 4 did not affect the lifetimes of serine-ligand interactions, but it did increase the amount of ligands engaging in an interaction of this type, as shown in Table 8. The olefination of the *sn*-2 chain in Bilayer 5 decreased amine-carboxylate lifetimes. Polyunsaturated fatty acids can increase head-group spacing between phospholipid and disrupt surface interactions,[63] but the decrease is not out of range of previous lifetimes, and the consistency of the phosphate-amide interaction does not suggest that lipid spacing is significantly affected.

Hydrogen bonding lifetimes fluctuate between 25.0 ns samples likely due to the fluctuation and clustering of phosphatidylserine. Both NAGly and serine contain hydrogen bond donors and anionic acceptors, so grouping of ligands and phosphatidylserine is common and can stabilize interactions, as shown in Figure 20. When clustered, a specific serine-ligand phosphate hydrogen bonding pair can persist more than half of the 25 ns sample, but more non-clustered ligands cannot access hydrogen bond partners and the average interaction lifetime is diminished compared to samples with evenly dispersed phosphatidylserine.

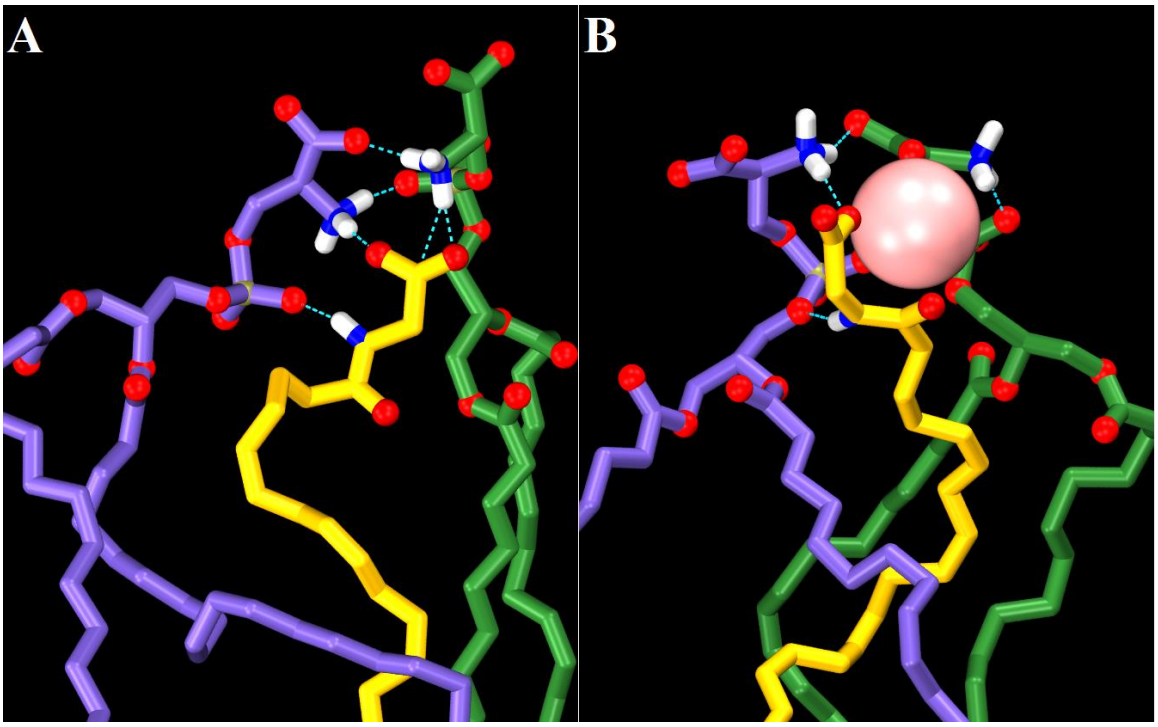

Figure 20. NAGly and Phosphatidylserine Interactions. (A) Hydrogen bonding networks and (B) sodium coordination. Oxygen shown in red, phosphorus in gold, nitrogen in blue, and polar hydrogens in white. NAGly carbons colored yellow and phosphatidylserine carbons colored violet or green to differentiate lipids. Sodium shown as a pink sphere. Hydrogen bonds shown in cyan. Nonpolar hydrogens omitted for clarity.

Phosphatidylethanolamine. Even as only a minor component of the extracellular leaflet, phosphatidylethanolamine hydrogen bonding lifetimes with NAGly remained consistent compared to the cytosolic leaflet, as shown in Table 6. Additionally, as shown in Table 8, all or most NAGly in Bilayers 2-5 interact with phosphatidylethanolamine in either leaflet, despite asymmetry in composition. Over Bilayers 2-5, phosphate-amide interaction lifetimes in extracellular and cytosolic leaflets remain fairly stable averaging 11.4 % and 14.5 %, respectively. Amine-carboxylate lifetimes averaged 36 % and 45 % in the extracellular and cytosolic leaflets, and glycerol-amine lifetimes averaged 2 %

between both leaflets; examples of both of these interactions are shown in Figure 21. A decrease is observed in the extracellular leaflet of Bilayer 3 due to sphingomyelin. Only minute changes in hydrogen bonding lifetimes were observed in Bilayers 3-5.

Complementary charges of ethanolamine and NAGly transpired clusters similar to those discussed for phosphatidylserine, especially in the cytosolic leaflet where phosphatidylethanolamine is the majority species. In one case, persistent hydrogen bonds with surrounding phosphatidylethanolamines trapped NAGly, as shown in Figure 21A.

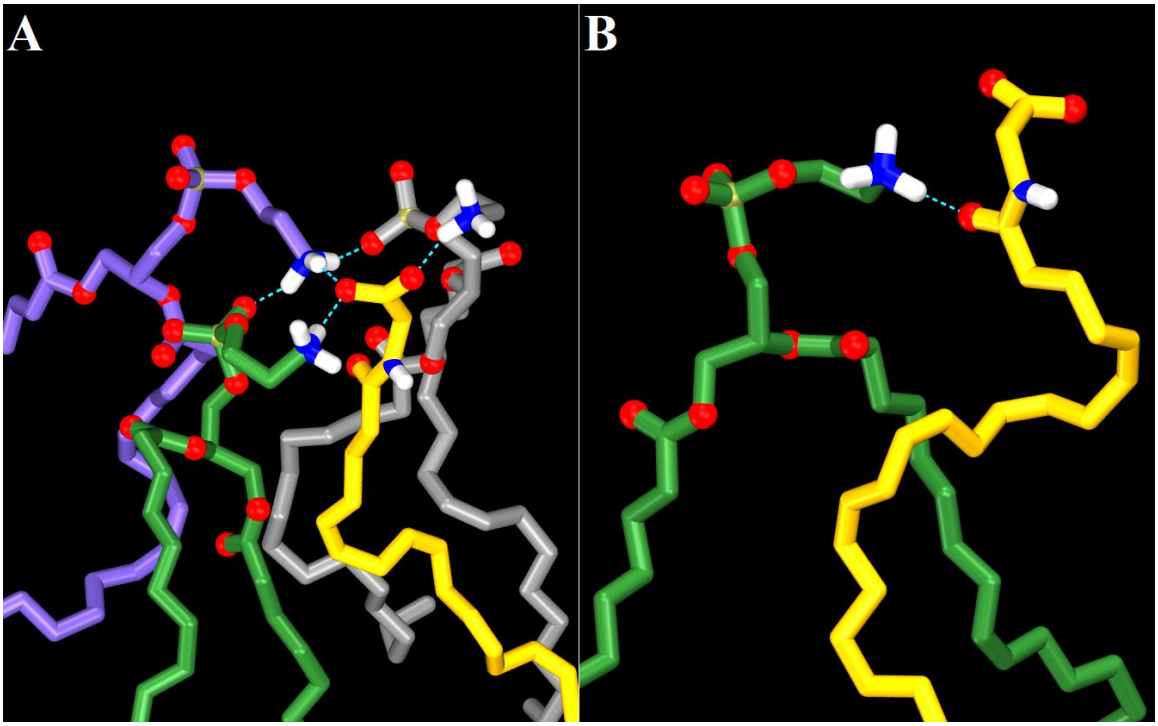

Figure 21. NAGly and Phosphatidylethanolamine Interactions. Hydrogen bonding networks between phosphatidylethanolamine and the (A) carboxylate and (B) amide of NAGly. Oxygens shown in red, phosphorus in gold, nitrogen in blue, and polar hydrogens in white. Phophsatidylethanolamine carbons colored green, violet or cyan, according to different lipids. NAGly carbons colored yellow Hydrogen bonds shown in green dash. Nonpolar hydrogens omitted for clarity.

Phosphatidylinositol. Only four inositol-4,5-biphosphate lipids were included in a cytosolic leaflet, and only a few hydrogen bonding pairs with NAGly were observed in Bilayers 3-5. When the inositol ring was tilted parallel to the membrane interface, interactions between the protonated inositol phosphate and a ligand carboxylate persisted for over ten nanoseconds, as shown in Figure 22A. The addition of cholesterol and polyunsaturated fatty acids did not significantly affect ligand interactions with inositol phospholipids, as they were rare previously. In another simulation a ligand molecule was trapped beneath two phosphatidylinositol-4,5-biphosphates for more than 4 ns, as shown in Figure 22B.

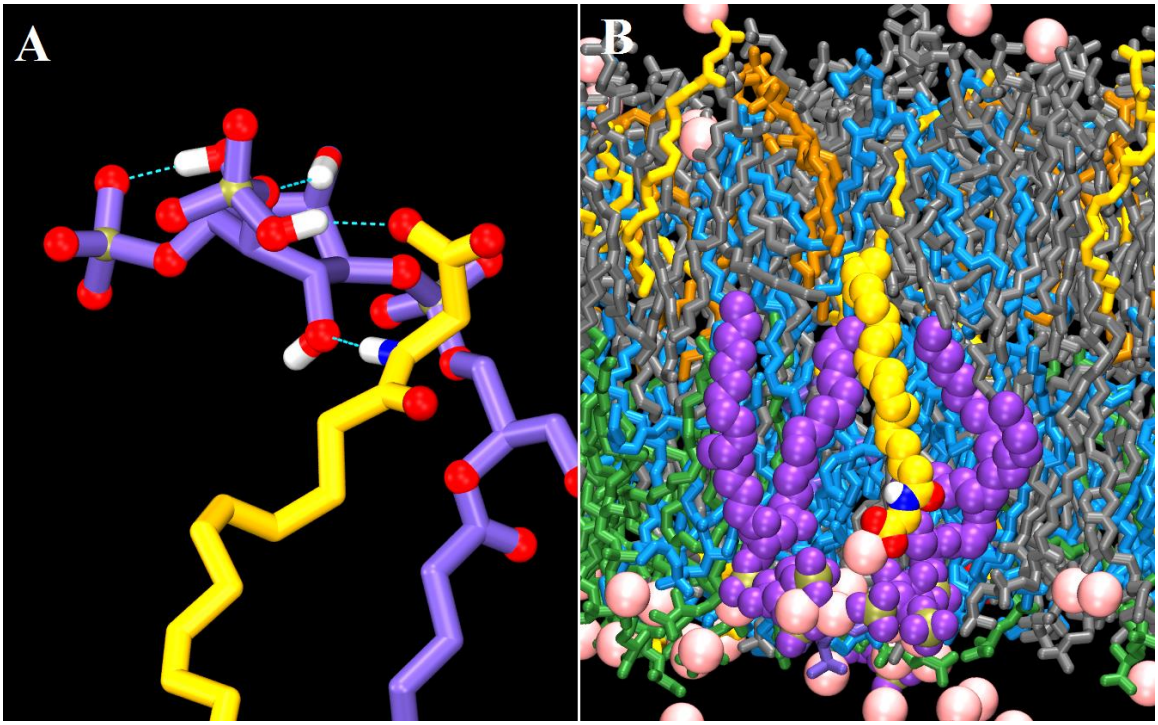

Figure 22. NAGly and Phosphatidylinositol-4,5-biphosphate Interactions. (A) Example of hydrogen bonding, shown by a green dash. (B) Example of two phosphatidylinositol-4,5-biphosphates trapping NAGly underneath a series of sodium ions. Oxygens shown in red, phosphorus in brown, nitrogen in blue, and polar hydrogens in white. Ligand and phospholipids carbons shown in yellow and violet, respectively. Hydrogen bonds shown by a green dash. Nonpolar hydrogens omitted for clarity.

Sphingomyelin. As shown in Table 6, phosphate-amide interactions between sphingomyelin and NAGly were less likely than others, present only about 6 % of a sample. Only 1-3 ligands would hydrogen bond with sphingomyelin over a 25 ns sample, as shown in Table 8. Ceramide donor hydroxyl and ligand amide carbonyls are positioned favorably in the bilayer to interact similarly to the example shown in Figure 23; this interaction was present 15 % of one ligand sample trajectory. Interestingly, the seemingly simple reversal of the donor-acceptor pair (sphingomyelin carbonyl and NAGly amide)

was present less than 1% of a given NAGly trajectory in Bilayers 4 and 5, suggesting a preference for orientation between the two molecules. Even more interesting, in Bilayer 3 these bonding lifetimes are more evenly distributed than in Bilayer 4; this suggests the preference seen between sphingomyelin and NAGly could be an artifact of a preference for orientation with cholesterol. The addition of cholesterol to the membrane with more saturated phospholipids further decreased the likelihood of these interactions, and the addition of polyunsaturated fatty acids only slightly increased average percentage lifetimes.

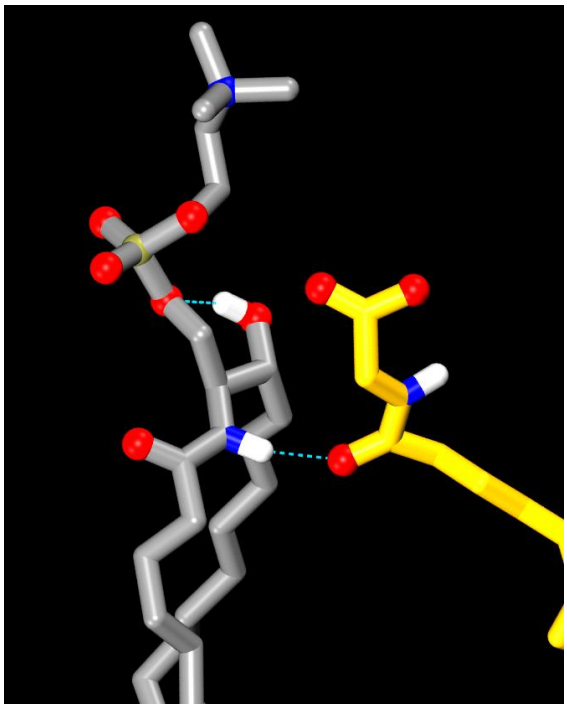

Figure 23. NAGly and Sphingomyelin Interactions. Oxygens shown in red, phosphorus in gold, nitrogen in blue, and polar hydrogens in white. Ligand and phospholipids carbons shown in yellow and cyan, respectively. Hydrogen bonds shown by a green dash. Nonpolar hydrogens omitted for clarity.

Cholesterol. NAGly is highly olefinated, and a not a minor component of a leaflet, so an intrinsic increase in the fluidity of the bilayer is expected. Increased fluidity in the hydrophobic core increases the likelihood of cholesterol tilting and completing a flip-flop. This is supported by the lack of flip-flop events observed in an equivalent composition to Bilayer 5 lacking ligands (see Appendix A). Several NAGly played a role in the canonical cholesterol flip-flop introduced in Figure 14 of Chapter III. The steroid completed the transition to the cytosolic leaflet when the hydroxyl hydrogen bonded with a cluster of ligands and anchored the steroid into the disordered center of the group, as shown in Figure 24. This complicates conclusions made about membrane molecular dynamics in general, suggesting that not only the membrane composition of neurons, but also any endogenous lipophilic ligands in a high concentration, can alter membrane properties.

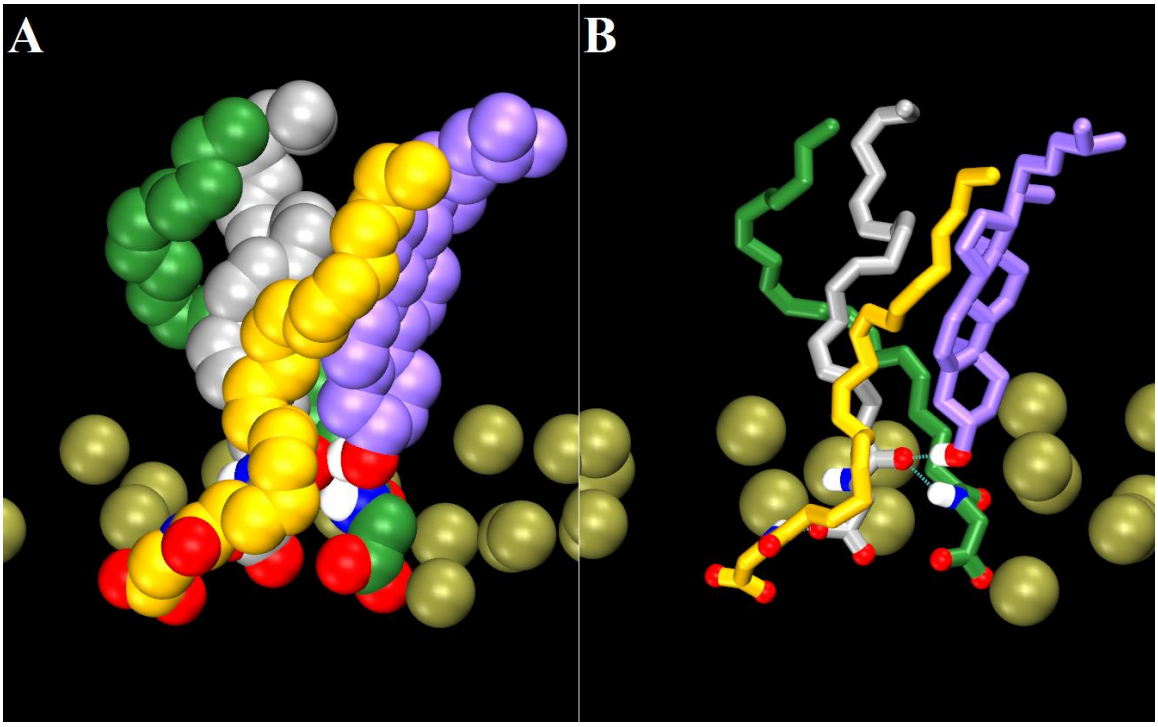

Figure 24. NAGly in Cholesterol Flip-flop. A ligand cluster anchoring cholesterol in (A) van der Waals representation, and (B) Licorice representation. Hydrogen bonds shown in cyan dash, cholesterol carbons colored violet, NAGly carbons colored yellow, silver, or green to differentiate lipids. Oxygen colored red, nitrogen colored blue, phosphorus in gold spheres, and polar hydrogen is white. Nonpolar hydrogens omitted for clarity.

Summary & Future Directions

In various leaflet compositions, NAGly hydrogen bonds similarly with individual phospholipid species. Generally, cholesterol does not hydrogen bond with NAGly, and when they do occur the interactions are short-lived. Neither the addition of cholesterol nor the olefination of select phospholipids greatly affected the interaction lifetime of ligands and phospholipids. The lack of significant variation supports that cholesterol only weakly affects intermolecular hydrogen bonding at the membrane surface, despite its effects on lipid order and fluidity.[63]

Hurst et al., 2009 showed that a lipid portal exists in CB2, and upon ligand entry the receptor activates.[37] These simulations were calculated in a single-component bilayer, so the role of membrane surface interactions is unclear, and is of interest to pursue. Other researchers have investigated neurotransmitters and other small molecules interacting with membranes, as previous mentioned. Several cases of ligands being pushed towards the center of the bilayer were observed, involving both phospholipids and sodium ions. Biologically, these are possible mechanisms to isolate NAGly from water, promote transition into the hydrophobic core, and consequently reach the lipid portal found in CB2 receptors.

At physiological pH, the pKa of ligand carboxylates has been postulated to change at the water interface,[64] and these local changes mean that some NAGly ligands could be protonated rather than charged. Currently, the Reggio group is pursuing the replication of specific lipid compositions to include the protonated form of NAGly and investigate changes in the behavior discussed herein. The diffusion constant of NAGly in various membrane compositions is being pursued, however there are intrinsic issues with this calculation associated with simulation box size and periodic boundary conditions. Thus, this investigation is ongoing to ensure accurate calculation prior to reporting.

REFERENCES

1. Singer, S. J. & Nicolson, G. L. The Fluid Mosaic Model of the Structure of Cell Membranes. *Science* **175,** 720–731 (1972).
2. Poger, D. & Mark, A. E. Effect of Ring Size in ω-Alicyclic Fatty Acids on the Structural and Dynamical Properties Associated with Fluidity in Lipid Bilayers. *Langmuir* **31,** 11574–11582 (2015).
3. Monje-Galvan, V. & Klauda, J. B. Modeling Yeast Organelle Membranes and How Lipid Diversity Influences Bilayer Properties. *Biochemistry* **54,** 6852–6861 (2015).
4. van Meer, G., Voelker, D. R. & Feigenson, G. W. Membrane lipids: Where They Are and How They Behave. *Nat. Rev. Mol. Cell Biol.* **9,** 112–124 (2008).
5. Andoh, Y., Aoki, N. & Okazaki, S. Molecular Dynamics Study of Lipid Bilayers Modeling the Plasma Membranes of Mouse Hepatocytes and Hepatomas. *J. Chem. Phys.* **144,** 85104 (2016).
6. Verkleij, A. J. *et al.* The Asymmetric Distribution of Phospholipids in the Human Red Cell Membrane. *BBA - Biomembr.* **323,** 178–193 (1973).
7. Breckenrldge, W. C., Gombos, G. & Morgan, I. G. The Lipid Composition of Adult Rat Brain Synaptosomal Plasma Membranes. *Biochim. Biophys. Acta* **266,** 695–707 (1972).

8. Cotman, C. W., Blank, M., Moehl, A. & Snyder, F. Lipid Composition of Synaptic Plasma Membranes Isolated from Rat Brain by Zonal Centrifugation. *Biochemistry* **8,** 4606–4612 (1969).

9. Lafourcade, M. *et al.* Nutritional omega-3 Deficiency Abolishes Endocannabinoid-Mediated Neuronal Functions. *Nat. Neurosci.* **14,** 345–50 (2011).

10. Meyer, J. S. & Quenzer, L. F. *Psychopharmacology: Drugs, the Brain, and Behavior*. (2005).

11. Hauser, H., Pascher, I., Pearson, R. H. & Sundell, S. Preferred Conformation and Molecular Packing of Phosphatidylethanolamine and Phosphatidylcholine. *BBA - Rev. Biomembr.* **650,** 21–51 (1981).

12. Browning, J. L. Motions and Interactions of Phospholipid Head Groups at the Membrane Surface. 3. Dynamic Properties of Amine-Containing Head Groups. *Biochemistry* **20,** 7144–7151 (1981).

13. Suits, F., Pitman, M. C. & Feller, S. E. Molecular Dynamics Investigation of the Structural Properties of Phosphatidylethanolamine Lipid Bilayers. *J. Chem. Phys.* **122,** 244714 (2005).

14. Luckey, M. *Membrane Structural Biology with Biochemical and Biophysical Foundations*. (2008).

15. Maekawa, M. & Fairn, G. D. Complementary Probes Reveal that Phosphatidylserine is Required for the Proper Transbilayer Distribution of Cholesterol. *J. Cell Sci.* **128,** 1422–33 (2015).

16. Yeung, T. *et al.* Membrane Phosphatidylserine Regulates Surface Charge and Protein Localization. *Science (80-.).* **319,** 210 LP-213 (2008).

17. Fairn, G. D. & Grinstein, S. Precursor or Charge Supplier? *Science (80-.).* **337,** 653–654 (2012).

18. Khelashvili, G. *et al.* Computational Modeling of the N-terminus of the Human Dopamine Transporter and its Interaction with PIP2-containing Membranes. *Proteins Struct. Funct. Bioinforma.* **83,** 952–969 (2015).

19. Lupyan, D., Mezei, M., Logothetis, D. E. & Osman, R. A Molecular Dynamics Investigation of Lipid Bilayer Perturbation by PIP2. *Biophys. J.* **98,** 240–247 (2010).

20. Pitman, M. C., Suits, F., MacKerell, A. D. & Feller, S. E. Molecular-level Organization of Saturated and Polyunsaturated Fatty Acids in a Phosphatidylcholine Bilayer Containing Cholesterol. *Biochemistry* **43,** 15318–15328 (2004).

21. Huber, T., Rajamoorthi, K., Kurze, V. F., Beyer, K. & Brown, M. F. Structure of docosahexaenoic acid-containing phospholipid bilayers as studied by 2H NMR and molecular dynamics simulations. *J. Am. Chem. Soc.* **124,** 298–309 (2002).

22. Lingwood, D. & Simons, K. Lipid rafts as a membrane-organizing principle. *Science* **327,** 46–50 (2010).

23. Huster, D., Arnold, K. & Gawrisch, K. Influence of Docosahexaenoic Acid and Cholesterol on Lateral Lipid organization in Phospholipid Mixtures. *Biochemistry* **37,** 17299–17308 (1998).

24. Leftin, A., Molugu, T. R., Job, C., Beyer, K. & Brown, M. F. Area per Lipid and Cholesterol Interactions in Membranes from Separated Local-field 13C NMR Spectroscopy. *Biophys. J.* **107,** 2274–2286 (2014).

25. Harroun, T. A., Katsaras, J. & Wassall, S. R. Cholesterol is Found to Reside in the Center of a Polyunsaturated Lipid Membrane. *Biochemistry* **47,** 7090–7096 (2008).

26. Kucerka, N. *et al.* The Effect of Cholesterol on Short- and Long-chain Monounsaturated Lipid Bilayers as Determined by Molecular Dynamics Simulations and X-ray Scattering. *Biophys. J.* **95,** 2792–2805 (2008).

27. Marrink, S. J., De Vries, A. H., Harroun, T. A., Katsaras, J. & Wassall, S. R. Cholesterol Shows Preference for the Interior of Polyunsaturated Lipid Membranes. *J. Am. Chem. Soc.* **130,** 10–11 (2008).

28. Dai, J., Alwarawrah, M. & Huang, J. Instability of Cholesterol cClusters in Lipid Bilayers and the Cholesterol's Umbrella Effect. *J. Phys. Chem. B* **114,** 840–848 (2010).

29. Bennett, W. F. D., MacCallum, J. L., Hinner, M. J., Marrink, S. J. & Tieleman, D. P. Molecular view of Cholesterol Flip-flop and Chemical Potential in Different Membrane Environments. *J. Am. Chem. Soc.* **131,** 12714–12720 (2009).

30. Ingólfsson, H. I. *et al.* Lipid Organization of the Plasma Membrane Lipid Organization of the Plasma Membrane. *J. Am. Chem. Soc.* **136,** 14554–14559 (2014).

31. Choubey, A., Kalia, R. K., Malmstadt, N., Nakano, A. & Vashishta, P. Cholesterol Translocation in a Phospholipid Membrane. *Biophys. J.* **104,** 2429–2436 (2013).

32. Venable, R. M., Luo, Y., Gawrisch, K., Roux, B. & Pastor, R. W. Simulations of Anionic Lipid mMembranes: Development of Interaction-specific Ion Parameters and Validation Using NMR Data. *J. Phys. Chem. B* **117,** 10183–10192 (2013).

33. Venable, R. M. *et al.* CHARMM All-atom Additive Force Field for Sphingomyelin: Elucidation of Hydrogen Bonding and of Positive Curvature. *Biophys. J.* **107,** 134–145 (2014).

34. Klauda, J. B., Monje, V., Kim, T. & Im, W. Improving the CHARMM Force Field for Polyunsaturated Fatty Acid Chains. *J. Phys. Chem. B* **116,** 9424–31 (2012).

35. Kotsikorou, E., Lynch, D. L., Abood, M. E. & Reggio, P. H. Lipid Bilayer Molecular Dynamics Study of Lipid-derived Agonists of the Putative Cannabinoid Receptor, GPR55. *Chem. Phys. Lipids* **164,** 131–143 (2011).

36. Lynch, D. L. & Reggio, P. H. Molecular Dynamics Simulations of the Endocannabinoid N-Arachidonoylethanolamine (Anandamide) in a Phospholipid Bilayer: Probing Structure and Dynamics. *J. Med. Chem.* **48,** 4824–4833 (2005).

37. Hurst, D. P. *et al.* A Lipid Pathway for Ligand Binding is Necessary for a Cannabinoid G protein-coupled Receptor. *J. Biol. Chem.* **285,** 17954–17964 (2010).

38. Kohno, M. *et al.* Identification of N-arachidonylglycine as the Endogenous Ligand for Orphan G-protein-coupled Receptor GPR18. *Biochem. Biophys. Res. Commun.* **347,** 827–832 (2006).

39. Whitnell, R. M., Hurst, D. P., Reggio, P. H. & Guarnieri, F. Conformational Memories with Variable Bond Angles. *J. Comput. Chem.* **29,** 741–752 (2008).

40. Barnett-Norris, J., Guarnieri, F., Hurst, D. P. & Reggio, P. H. Exploration of Biologically Relevant Conformations of Anandamide, 2-arachidonylglycerol, and Their Analogues Using Conformational Memories. *J. Med. Chem.* **41,** 4861–4872 (1998).

41. Konas, R. M., Daristotle, J. L., Harbor, N. B. & Klauda, J. B. Biophysical Changes of Lipid Membranes in the Presence of Ethanol at Varying Concentrations. *J. Phys. Chem. B* **119,** 13134–13141 (2015).

42. Zapata-Morin, P. A., Sierra-Valdez, F. J. & Ruiz-Suárez, J. C. The Interaction of Local Anesthetics with Lipid Membranes. *J. Mol. Graph. Model.* **53,** 200–205 (2014).

43. Jarosaw Meller. Molecular Dynamics. *Encycl. Life Sci.* 1–8 (2001). doi:10.1021/jp909004y

44. Adcock, S. a & Mccammon, J. A. Molecular Dynamics : Survey of Methods for Simulating the Activity of Proteins. *Chem. Rev.* **106,** 1589–1615 (2006).

45. Tieleman, D. ., Marrink, S. . & Berendsen, H. J. . A Computer Perspective of Membranes: Molecular Dynamics Studies of Lipid Bilayer Systems. *Biochim. Biophys. Acta - Rev. Biomembr.* **1331,** 235–270 (1997).

46. Lee, J. *et al.* CHARMM-GUI Input Generator for NAMD, GROMACS, AMBER, OpenMM, and CHARMM/OpenMM Simulations Using the CHARMM36 Additive Force Field. *J. Chem. Theory Comput.* **12,** 405–413 (2016).

47. Phillips, J. C. *et al.* Scalable Molecular Dynamics with NAMD. *J. Comput. Chem.* **26,** 1781–1802 (2005).

48. Essman, U. *et al.* A Smooth Particle Mesh Ewald Method. *J. Chem. Phys.* **103,** 8577–8593 (1995).

49. Humphrey, W., Dalke, A. & Schulten, K. VDM: Visual Molecular Dynamics. *J. Mol. Graph.* **14,** 33–8, NaN, 27–28 (1996).

50. Romo, T. D., Leioatts, N. & Grossfield, A. Lightweight Object Oriented Structure Analysis: Tools for Building Tools to Analyze Molecular Dynamics Simulations. *J. Comput. Chem.* **35,** 2305–2318 (2014).

51. Lukat, G., Kruger, J. & Sommer, B. APL@Voro: A Voronoi-Based Membrane Analysis Tool for GROMACS Trajectories. *J. Chem. Inf. Model.* **53,** 2908–2925 (2013).

52. Vermeer, L. S., De Groot, B. L., Réat, V., Milon, A. & Czaplicki, J. Acyl Chain Order Parameter Profiles in Phospholipid Bilayers: Computation from Molecular Dynamics Simulations and Comparison with 2H NMR Experiments. *Eur. Biophys. J.* **36,** 919–931 (2007).

53. Janosi, L. & Gorfe, A. A. Simulating POPC and POPC/POPG bilayers: Conserved Packing and Altered Surface Reactivity. *J. Chem. Theory Comput.* **6,** 3267–3273 (2010).

54. Poger, D. & Mark, A. E. On the Validation of Molecular Dynamics Simulations of Saturated and cis -Monounsaturated Phosphatidylcholine Lipid Bilayers: A Comparison with Experiment. *J Chem Theory Comput* **6,** 325–336 (2010).

55. Pyrkova, D. D. V *et al.* Dynamic Clustering of Lipids in Hydrated Two-component Membranes: Results of Computer Modeling and Putative Biological Impact. *J. Biomol. Struct. Dyn.* **31,** 87–95 (2013).

56. Jurkiewicz, P., Cwiklik, L., Vojtíšková, A., Jungwirth, P. & Hof, M. Structure, Dynamics, and Hydration of POPC/POPS bilayers Suspended in NaCl, KCl, and CsCl Solutions. *Biochim. Biophys. Acta - Biomembr.* **1818,** 609–616 (2012).

57. Boettcher, J. M. *et al.* Atomic View of Calcium-Induced Clustering of Phosphatidylserine in Mixed Lipid Bilayers. *Biochemistry* **50,** 2264–2273 (2011).

58. Brown, D. A. PIP2 Clustering: From Model Membranes to Cells. *Chem. Phys. Lipids* **192,** 33–40 (2015).

59. Kučerka, N. *et al.* Molecular Structures of Fluid Phosphatidylethanolamine Bilayers Oobtained from Simulation-to-experiment Comparisons and Experimental Scattering Density Profiles. *J. Phys. Chem. A* **119,** 1947–1956 (2015).

60. Boggs, J. M., Rangaraj, G. & Koshy, K. M. Effect of Hydrogen-bonding and Non-hydrogen-bonding Long Chain Compounds on the Phase Transition Temperatures of Phospholipids. *Chem. Phys. Lipids* **40,** 23–34 (1986).

61. Boggs, J. M. Lipid Intermolecular Hydrogen Bonding: Influence on Structural Organization and Membrane Function. *BBA - Rev. Biomembr.* **906,** 353–404 (1987).

62. Wu, E. L., Qi, Y., Song, K. C., Klauda, J. B. & Im, W. Preferred Orientations of Phosphoinositides in Bilayers and Their Implications in Protein Recognition Mechanisms. *J. Phys. Chem. B* **118,** 4315–4325 (2014).

63. Slater, S. J., Ho, C., Taddeo, F. J., Kelly, M. B. & Stubbs, C. D. Contribution of Hydrogen Bonding to Lipid-lipid Interactions in Membranes and the Role of Lipid Order: Effects of Cholesterol, Increased Phospholipid Unsaturation, and Ethanol. *Biochemistry* **32,** 3714–3721 (1993).

64. Periole, X., Ceruso, M. A. & Mehler, E. L. Acid-base Equilibria in Rhodopsin: Dependence of the Protonation State of Glu134 on its Environment. *Biochemistry* **43,** 6858–6864 (2004).

APPENDIX A

MEMBRANE COMPOSITIONS LACKING NAGLY

Table 9. Membrane Compositions Lacking NAGly. PC = Phosphatidylcholine, PE = Phosphatidylethanolamine, SM = Sphingomyelin, PS = phosphatidylserine, PIP2 = phosphatidylinositol-4,5-biphosphate, and CHL = cholesterol. Values provided are mole percentages of the total lipid in the bilayer. Symmetric refers to equivalent mole percentages of a specific phospholipid between bilayer leaflets, while asymmetric refers to an unequal distribution between leaflets.

NAGly Equivalent Bilayer	Leaflet	PC	PE	SM	PS	PIP2	CHL
0	**Extra**	*100.00%*	-	-	-	-	-
	Cytosolic	*100.00%*	-	-	-	-	-
	Total	*100.00%*	-	-	-	-	-
1 Symmetric	**Extra**	*80.00%*	-	-	*20.00%*	-	-
	Cytosolic	*80.00%*	-	-	*20.00%*	-	-
	Total	*80.00%*	-	-	*20.00%*	-	-
1 Asymmetric	**Extra**	*100.00%*	-	-	-	-	-
	Cytosolic	*80.00%*	-	-	*20.00%*	-	-
	Total	*89.88%*	-	-	*10.12%*	-	-
2 Symmetric	**Extra**	*66.67%*	*33.33%*	-	-	-	-
	Cytosolic	*47.73%*	*31.82%*	-	*20.45%*	-	-
	Total	*57.09%*	*32.57%*	-	*10.34%*	-	-
2 Asymmetric	**Extra**	*83.33%*	*16.67%*	-	-	-	-
	Cytosolic	*33.33%*	*46.67%*	-	*20.00%*	-	-
	Total	*57.47%*	*32.18%*	-	*10.34%*	-	-
3	**Extra**	*72.31%*	*20.00%*	*7.69%*	-	-	-
	Cytosolic	*33.09%*	*43.38%*	-	*20.59%*	*2.94%*	-
	Total	*52.26%*	*31.95%*	*3.76%*	*10.53%*	*1.50%*	-
4	**Extra**	*61.03%*	*19.12%*	*7.35%*	-	-	*12.50%*
	Cytosolic	*23.94%*	*41.55%*	-	*19.72%*	*2.82%*	*11.97%*
	Total	*42.09%*	*30.58%*	*3.60%*	*10.07%*	*1.44%*	*12.23%*
5	**Extra**	*62.32%*	*18.84%*	*7.25%*	-	-	*11.59%*
	Cytosolic	*21.43%*	*42.86%*	-	*20.00%*	*2.86%*	*12.86%*
	Total	*41.73%*	*30.94%*	*3.60%*	*10.07%*	*1.44%*	*12.23%*

APPENDIX B

HYDROGEN BONDING LIFETIMES OF SAMPLES

Interaction lifetimes between ligands and phospholipids of the 25 ns samples discussed in Chapter IV are presented here. Table 10 shows the common phospholipids-NAGly hydrogen bonding pair data, and Table 11 shows the lifetime data for pairs not including phospholipid phosphate or glycerol oxygens. These values were averaged to produce Table 6.

Table 10. Detailed Interaction Lifetimes: Phosphate and Glycerol Oxygens. PO4 = phosphate, O–C=O = glycerol oxygens, and NH = NAGly+ amide proton. Lifetime values are a percentages of a 25 ns sample trajectory (samples a-d). An asterisk indicates a phospholipid-ligand bonding pair.

PC-NAGly		**PO4 * NH**				**O–C=O * NH**			
Extracellular Leaflet	**Bilayer**	Sample a	Sample b	Sample c	Sample d	Sample a	Sample b	Sample c	Sample d
	1	24.00	24.03	21.33	22.83	4.07	4.10	3.97	3.27
	2	13.23	16.80	18.71	18.43	6.73	2.87	2.53	2.37
	3	11.04	12.28	12.43	13.11	2.48	2.84	3.60	5.69
	4	20.17	15.27	8.13	11.78	2.37	2.53	5.87	3.64
	5	12.74	15.16	13.38	13.82	1.73	3.16	4.22	5.09
Cytosolic Leaflet	**Bilayer**	Sample a	Sample b	Sample c	Sample d	Sample a	Sample b	Sample c	Sample d
	1	21.41	18.67	18.29	15.13	3.29	3.38	2.80	4.07
	2	12.80	11.52	11.85	11.65	1.68	0.72	1.30	2.80
	3	8.10	9.60	14.48	11.12	1.10	0.67	2.24	4.40
	4	10.40	5.07	6.64	11.60	0.80	0.73	0.24	1.40
	5	11.10	10.80	7.12	16.20	3.80	0.00	2.08	0.20
PS-NAGly		**PO4 * NH**				**O–C=O * NH**			
Cytosolic Leaflet	Bilayer	Sample a	Sample b	Sample c	Sample d	Sample a	Sample b	Sample c	Sample d
	1	25.09	14.17	11.16	11.72	4.17	4.57	0.80	0.64
	2	6.69	1.70	10.50	2.71	0.06	2.00	0.45	1.38
	3	6.20	2.23	8.20	13.49	1.00	1.54	4.60	1.89
	4	7.30	7.60	11.70	7.77	3.80	4.56	1.27	2.90
	5	7.89	13.53	6.32	2.00	4.11	3.93	4.88	3.90
PE-NAGly		**PO4 * NH**				**O–C=O * NH**			
Extracellular Leaflet	Bilayer	Sample a	Sample b	Sample c	Sample d	Sample a	Sample b	Sample c	Sample d
	2	6.73	15.25	21.51	13.68	0.80	1.25	1.20	2.60
	3	7.73	8.12	9.43	9.45	1.07	2.16	1.40	2.07
	4	11.32	7.91	10.49	12.23	1.69	2.46	1.29	1.33
	5	12.98	12.89	14.22	8.06	1.29	3.17	1.72	0.74
Cytosolic Leaflet	Bilayer	Sample a	Sample b	Sample c	Sample d	Sample a	Sample b	Sample c	Sample d
	2	15.47	14.63	18.13	15.80	1.93	2.67	2.50	2.80
	3	16.00	10.04	8.47	10.65	4.04	3.60	2.65	4.29
	4	18.06	14.52	10.06	17.13	3.02	1.48	3.26	2.07
	5	14.92	11.38	16.58	21.66	3.72	2.00	1.23	2.68
SM-NAGly		**PO4 * NH**							
Extracellular Leaflet	Bilayer	Sample a	Sample b	Sample c	Sample d				
	3	5.00	5.20	0.00	12.60				
	4	0.00	7.60	2.93	5.00				
	5	14.80	4.80	2.27	9.20				

Table 11. Detailed Interaction Lifetimes: Other Hydrogen Bonding Pairs. NH3 = primary amine, C=O = ligand amide carbonyl, COO = carboxylate, NH = amide proton of either NAGly or sphingomyelin, OH = sphingomyelin alcohol. Lifetime values are a percentages of a 25 ns sample trajectory (samples a-d). An asterisk indicates a phospholipid-ligand bonding pair.

PS-NAGly		**NH3 * COO**				**NH3 * C=O**			
Cytosolic Leaflet	Bilayer	Sample a	Sample b	Sample c	Sample d	Sample a	Sample b	Sample c	Sample d
	1	49.89	35.49	26.71	28.20	0.97	1.26	1.64	1.28
	2	21.26	20.80	18.45	14.89	0.23	2.70	1.90	1.24
	3	34.33	29.09	38.27	45.94	1.60	0.46	5.27	6.63
	4	42.23	24.73	31.10	35.03	2.17	0.98	0.90	0.30
	5	28.15	27.20	24.92	18.10	0.69	0.76	0.72	0.60
PE-NAGly		**NH3 * COO**				**NH3 * C=O**			
Extracellular Leaflet	Bilayer	Sample a	Sample b	Sample c	Sample d	Sample a	Sample b	Sample c	Sample d
	2	26.73	37.65	43.02	45.08	1.73	4.20	3.73	2.60
	3	26.40	28.56	26.00	29.82	2.31	2.04	2.63	2.29
	4	36.68	35.08	35.38	33.17	2.03	2.18	1.97	2.53
	5	39.09	42.46	42.15	44.49	2.77	3.51	2.92	2.49
Cytosolic Leaflet	Bilayer	Sample a	Sample b	Sample c	Sample d	Sample a	Sample b	Sample c	Sample d
	2	48.80	40.07	37.70	47.73	3.50	2.83	2.03	4.53
	3	52.76	39.31	45.53	35.75	2.68	3.20	3.64	2.20
	4	44.80	40.15	33.35	54.20	2.98	2.95	2.09	3.87
	5	48.95	49.75	47.02	52.62	3.51	2.31	2.46	2.92
SM-NAGly		**OH * NH**				**NH * C=O**			
Extracellular Leaflet	Bilayer	Sample a	Sample b	Sample c	Sample d	Sample a	Sample b	Sample c	Sample d
	3	0.40	0.40	9.60	0.00	3.20	11.87	6.93	1.40
	4	0.00	0.00	0.13	0.40	16.80	1.60	6.13	7.80
	5	1.60	0.00	0.00	0.00	0.00	31.20	18.27	3.80

APPENDIX C

SUPPLEMENTARY IMAGES

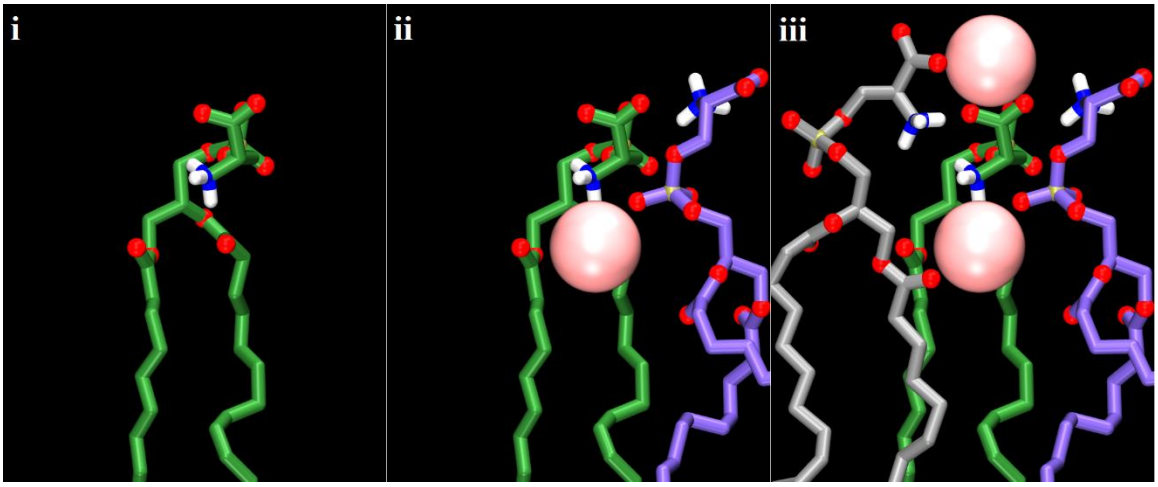

Figure 25. Supplemental Images of Figure 9B.

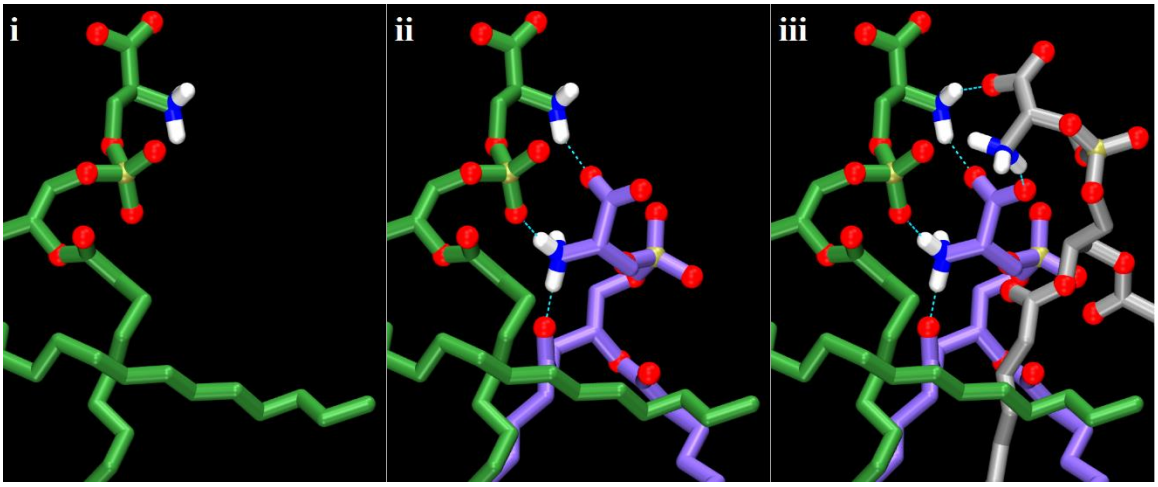

Figure 26. Supplemental Images of Figure 9C.

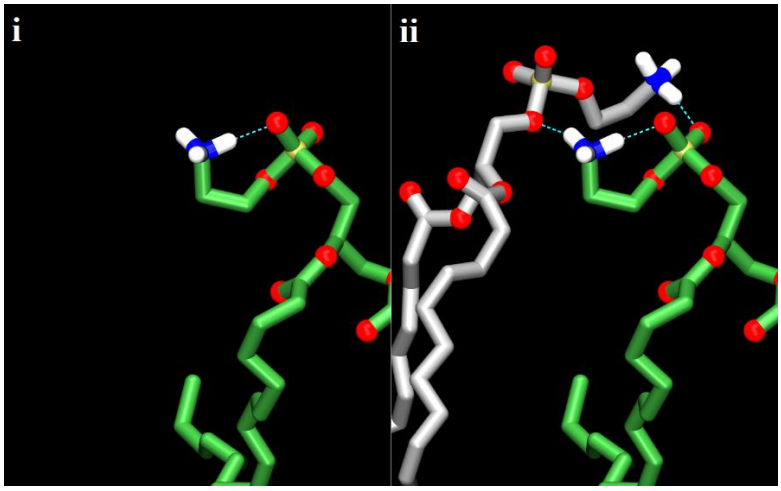

Figure 27. Supplemental Images of Figure 11A.

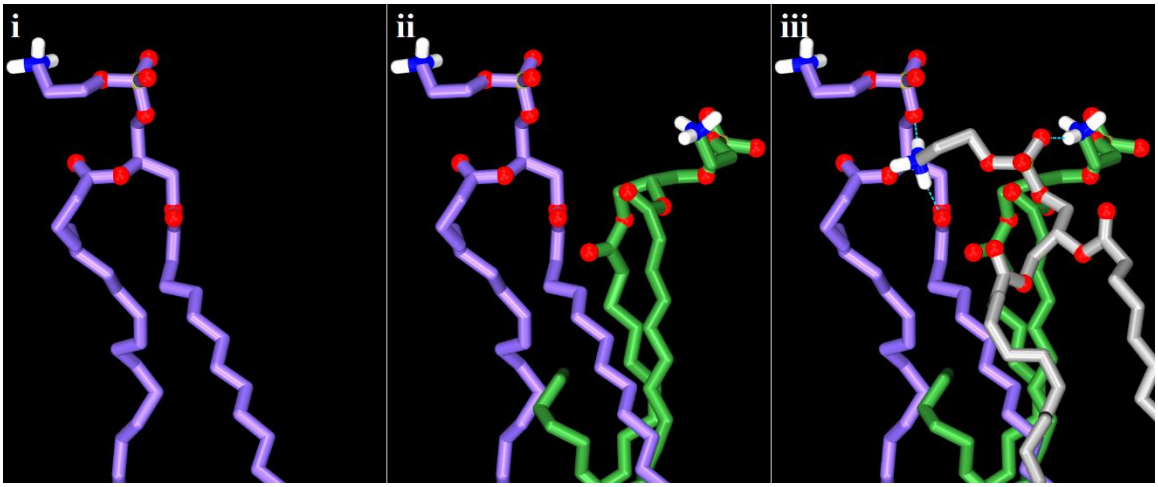

Figure 28. Supplemental Images of Figure 11B.

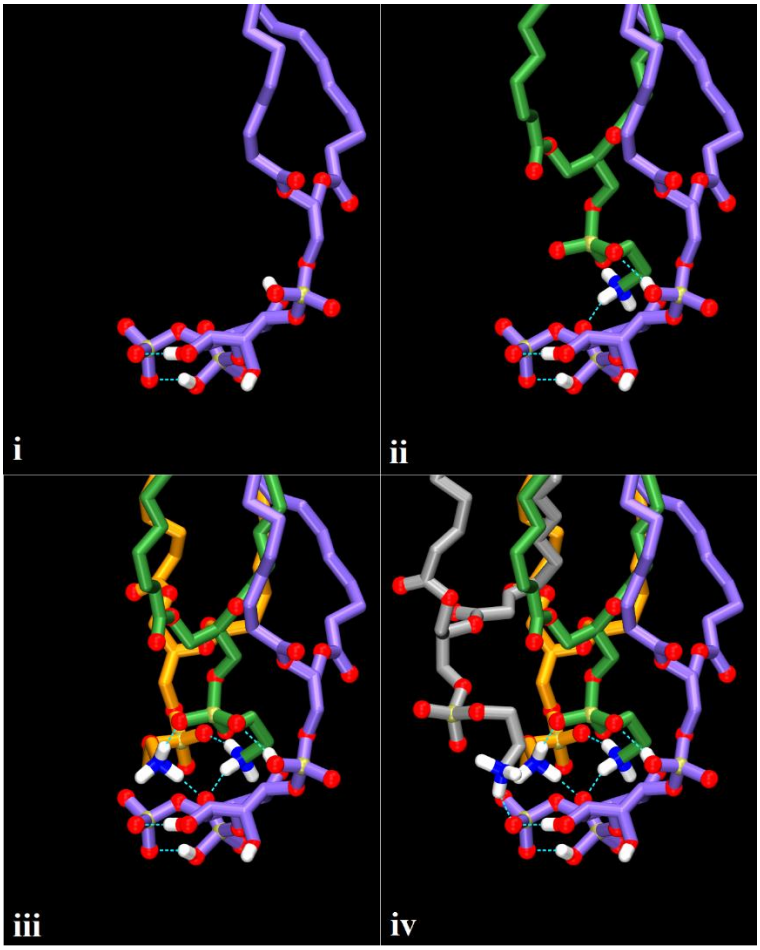

Figure 29. Supplemental Images of Figure 13A.

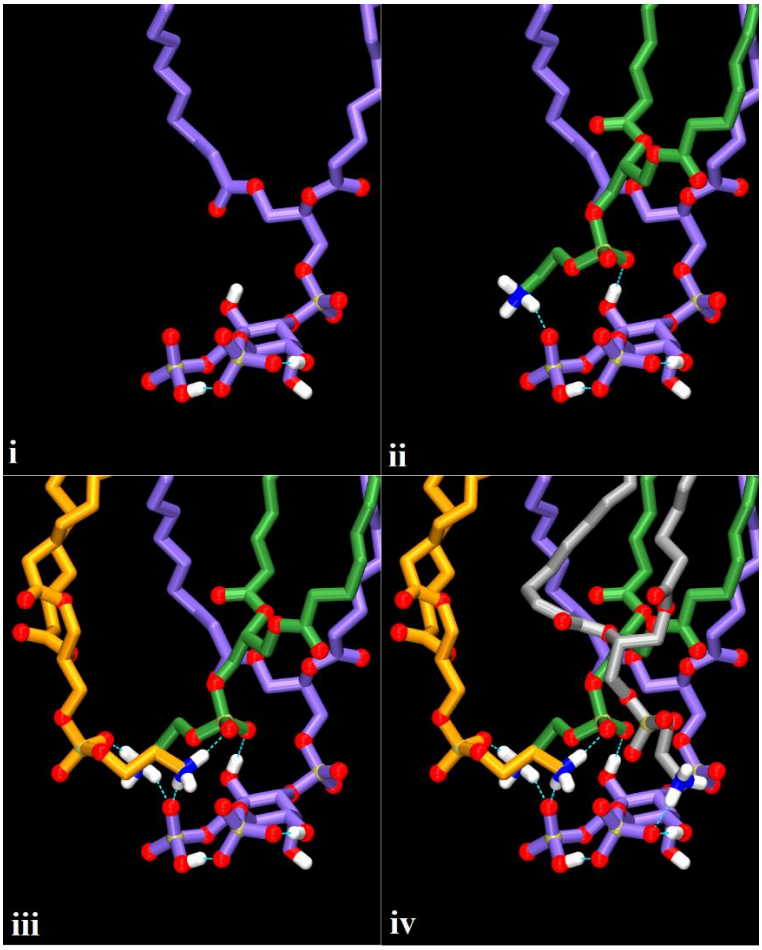

Figure 30. Supplemental Images of Figure 13B.

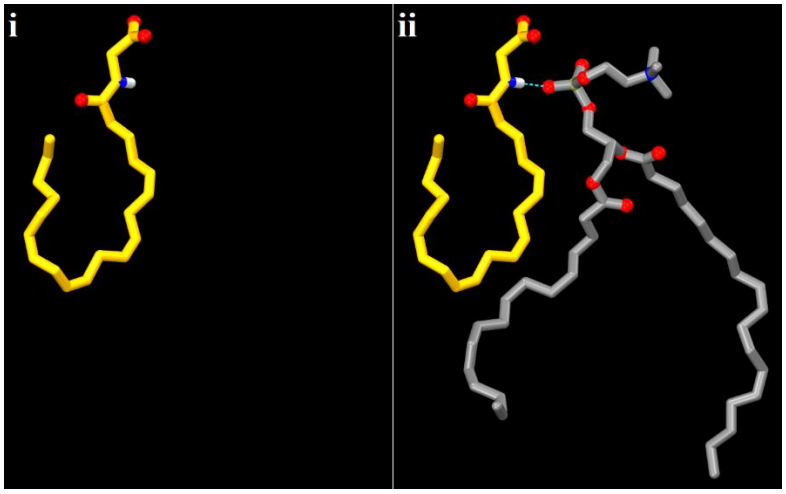

Figure 31. Supplemental Images of Figure 19A.

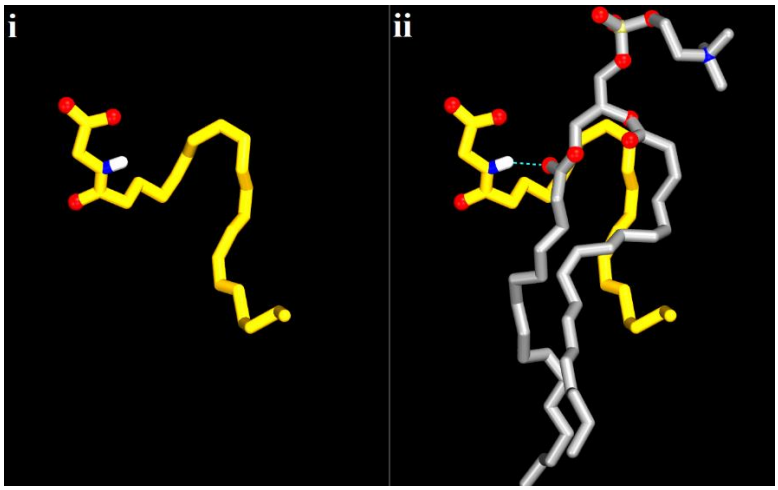

Figure 32. Supplemental Images of Figure 19B.

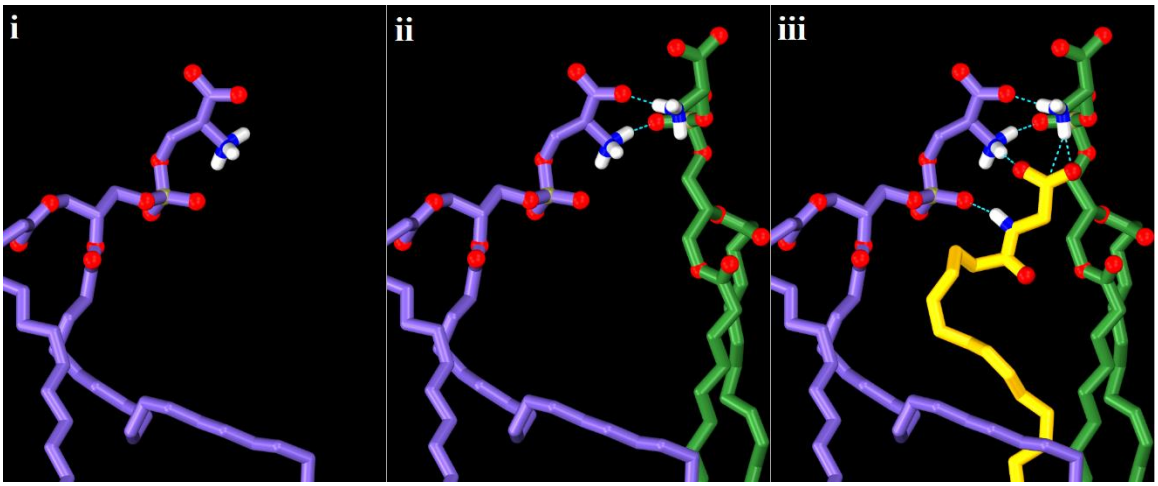

Figure 33. Supplemental Images of Figure 20A.

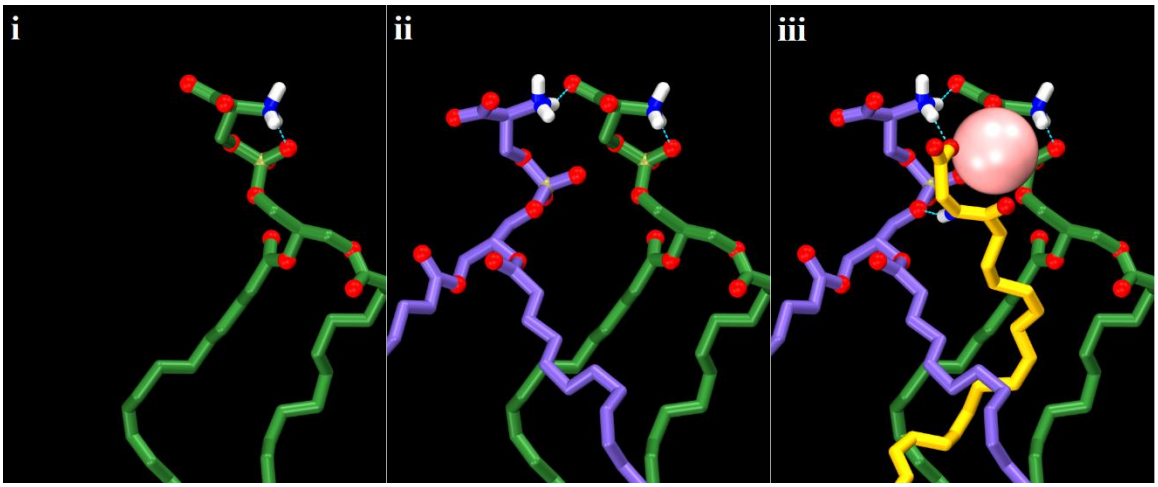

Figure 34. Supplemental Images of Figure 20B.

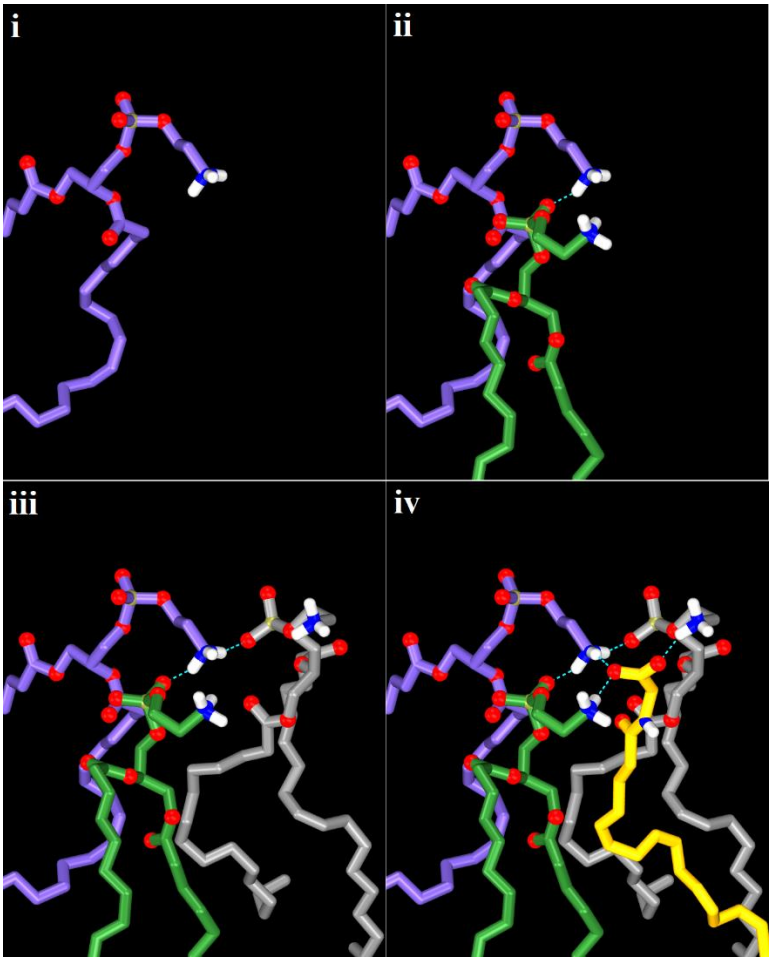

Figure 35. Supplemental Images of Figure 21A.

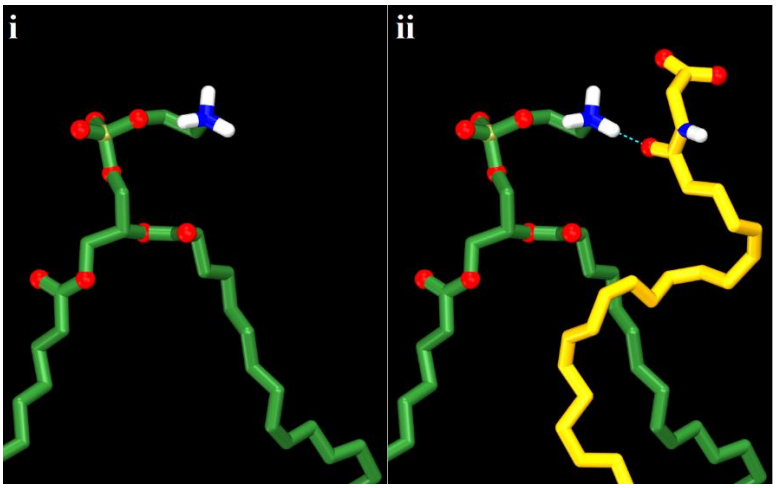

Figure 36. Supplemental Images of Figure 21B.

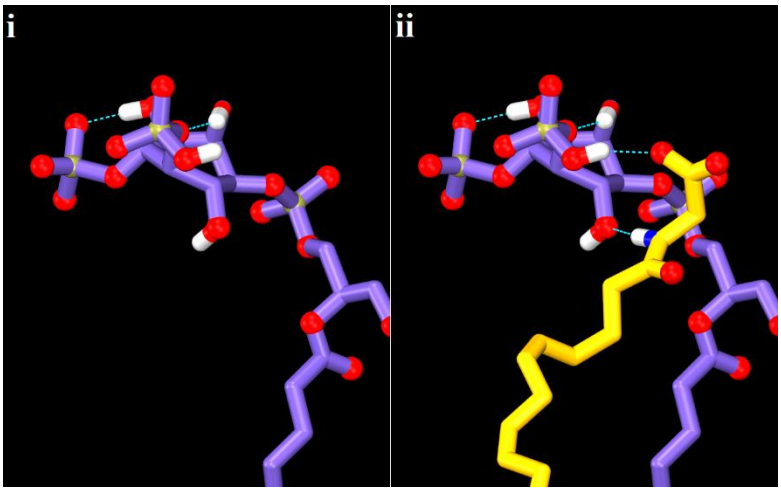

Figure 37. Supplemental Images of Figure 22A.

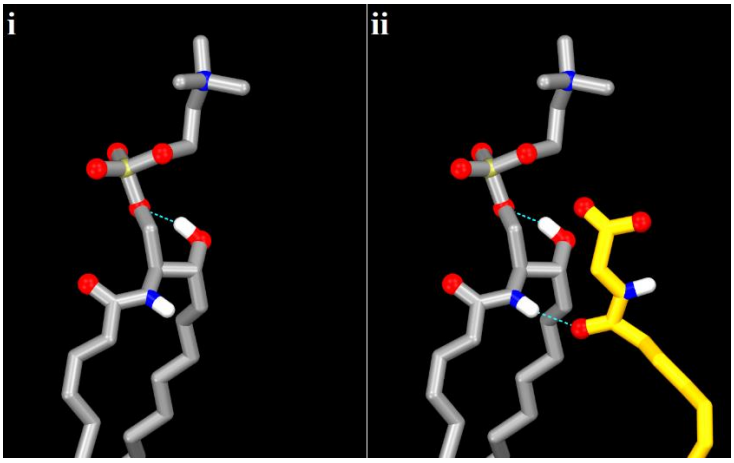

Figure 38. Supplemental Images of Figure 23.

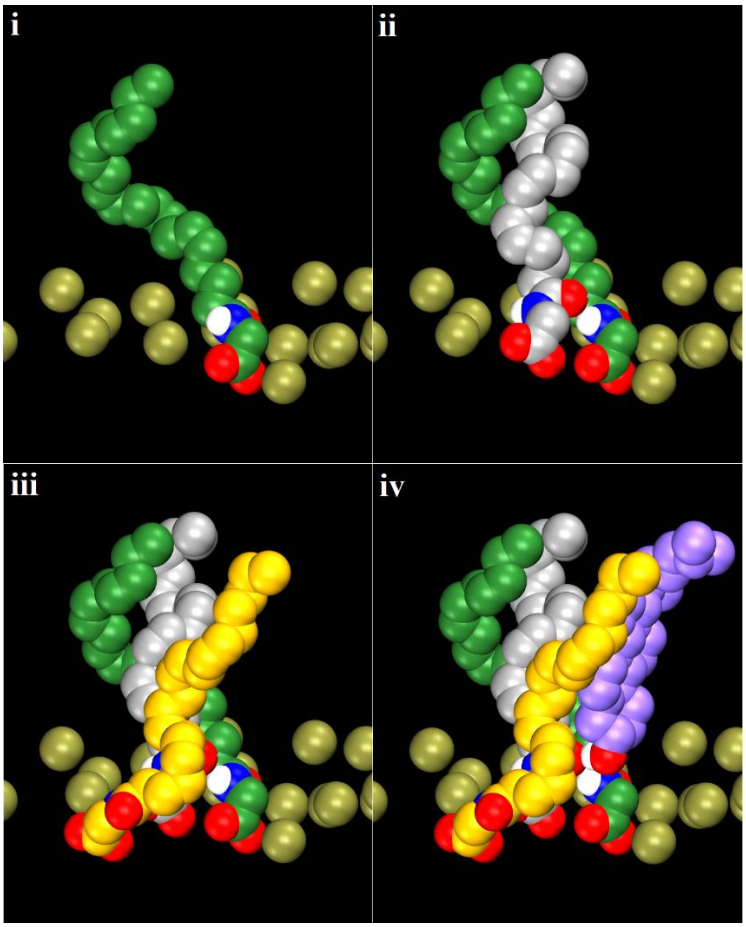

Figure 39. Supplemental Images of Figure 24A.

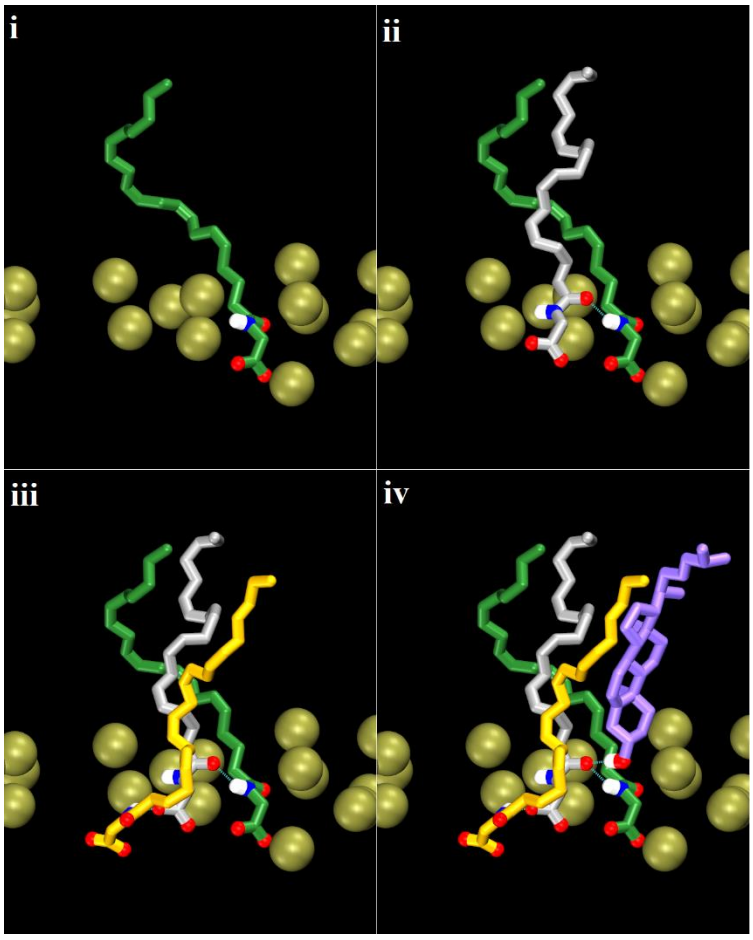

Figure 40. Supplemental Images of Figure 24B.